



HAL
open science

Hermite type Spline spaces over rectangular meshes with arbitrary topology

Meng Wu, Bernard Mourrain, André Galligo, Boniface Nkonga

► **To cite this version:**

Meng Wu, Bernard Mourrain, André Galligo, Boniface Nkonga. Hermite type Spline spaces over rectangular meshes with arbitrary topology. 2015. hal-01196428v2

HAL Id: hal-01196428

<https://inria.hal.science/hal-01196428v2>

Preprint submitted on 30 Nov 2015 (v2), last revised 25 Apr 2017 (v4)

HAL is a multi-disciplinary open access archive for the deposit and dissemination of scientific research documents, whether they are published or not. The documents may come from teaching and research institutions in France or abroad, or from public or private research centers.

L'archive ouverte pluridisciplinaire **HAL**, est destinée au dépôt et à la diffusion de documents scientifiques de niveau recherche, publiés ou non, émanant des établissements d'enseignement et de recherche français ou étrangers, des laboratoires publics ou privés.

Bicubic Spline spaces over rectangular meshes with arbitrary topologies

Meng Wu^{a,c,*}, Bernard Mourrain^a, André Galligo^b, Boniface Nkongha^b

^a*Galaad2, Inria, Sophia Antipolis, France*

^b*Lab. J. A. Dieudonné, University of Nice, Nice, France*

^c*School of Mathematics, Hefei University of Technology, P. R. China.*

Abstract

Motivated by the magneto hydrodynamic (MHD) simulation for Tokamaks with Iso-geometric analysis, we present a new type of spline space defined over a rectangular mesh with arbitrary topology, which is a spline space with bi-degree (d, d) and C^r parameter continuity. The main context of this paper is focused on the dimension formula, exhibiting basis functions called Hermite bases of a bicubic spline space and its potential applications to solving partial differential equations (PDEs) over a complex physical domain in the framework of Isogeometric analysis. Concretely, we analyze the property of parameterization, an approximation property with L^2 -norm, numerical convergence rates measured by L^2 -norm and H^1 -norm for solving the Grad-Shafranov equation by isogeometric techniques, and C^1 -continuity property of test functions that are composing the inverse of a parameterization in [28] with Hermite bases. Despite the fact that the basis functions are singular at extraordinary vertices, we show that the optimal approximation order and numerical convergence rates are reached. By analysing C^1 -continuity property, a C^1 -continuity constraint at extraordinary vertices is obtained and it preserves the optimal approximation order.

Keywords: Spline, Arbitrary topology meshes, Dimension and basis, Isogeometric analysis, MHD simulation

1. Introduction

The finite element method (FEM) is a powerful tool that is often used to derive accurate and robust scheme for the approximation of the solution of PDEs. We are concerned with MHD equations applied to the edge plasma of fusion devices as Tokamaks. In this context of strongly magnetized plasma, the finite element formulation

*Corresponding author at: Galaad2, INRIA Sophia-Antipolis, 2004 Route des Lucioles, 06902 Cedex, France; School of Mathematics, Hefei University of Technology, No. 193, Tunxi Road, Hefei, Anhui Prov., 230009, P. R. China.

Email addresses: meng.wu@hfut.edu.cn, wumeng@mail.ustc.edu.cn (Meng Wu), Bernard.Mourrain@inria.fr (Bernard Mourrain), andre.galligo@unice.fr (André Galligo), boniface.nkongha@unice.fr (Boniface Nkongha)

faces some difficulties such as the divergence-free constraint and the high anisotropy of transport processes. For applications to Tokamaks, the divergence-free constraint is enforced by the introduction of the potential vector: the magnetic field becomes the rotational of this vector. For the resistive MHD model, this leads to a system of partial differential equations of order greater than two. The weak formulations require test functions that are continuously differentiable (C^1), but because of the lack of smoothness (gradients are discontinuous), classical Lagrange finite elements cannot be directly applied.

On the other hand, higher anisotropies suggest the use of meshes aligned with the principal directions of the transport processes [1]. These directions are prescribed by the magnetic flux surfaces, and in this first approach, we assume that we are close to a given equilibrium so that the alignment can be achieved at the initial step. Unfortunately, for high-confinement Tokamaks, there is a saddle point, and the associated magnetic flux is singular. In this context, quadrilateral (2D) and hexahedral (3D) meshes are the most convenient for alignment and lead to a reduction in the approximation error. The construction of high-quality block structured meshes is a challenging issue when considering complex geometries, even if isoparametric finite elements [2] or isogeometric analysis [3] can help to fit on physically curved boundaries. For example, in our target application, to align the principal directions of the transport processes, a structured mesh is involved, as shown on the left side of Figure 2.

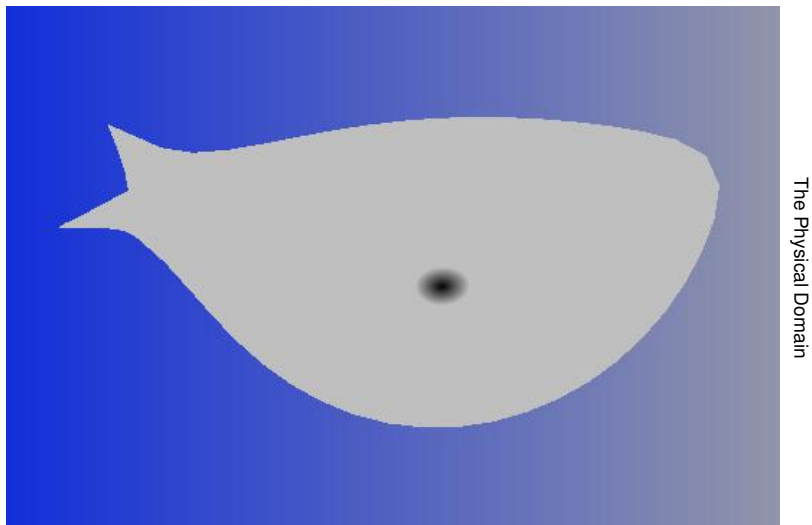


Figure 1: Physical domain of the target application

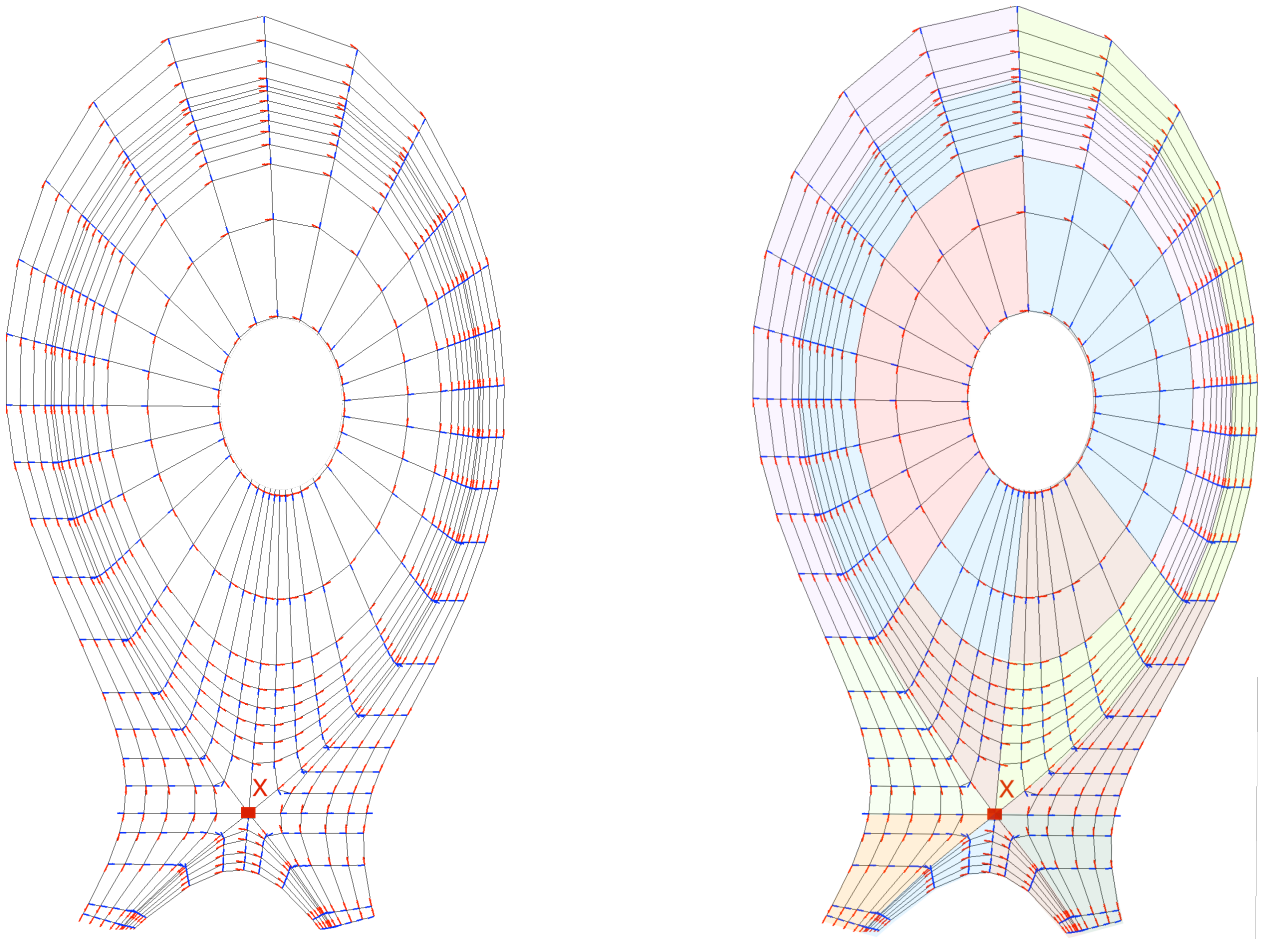


Figure 2: The structured mesh of the target application and its block structured mesh

Although tensor product B-splines [4], hierarchical B-splines [5],[6],[7], LR-splines [8] and T-splines [9] are often used as shape functions, they satisfy the parameter regularity requirement but their parametric domains are associated with simpler topological structures than that needed for our target applications. For example, the physical domains should be homeomorphic to rectangles because all of these splines are defined over rectangular parametric domains. In other words, the structured mesh on the left side of Figure 2 has to be decomposed when these splines are treated as shape functions. On the right side of Figure 2, we give an example of decomposition of the physical domain into a structured mesh. Splines defined over a manifold or a mesh with arbitrary topology are one way to avoid this decomposition problem.

Splines defined over a manifold are based on the classical definition of a differential manifold, see e.g. [10, 11, 12, 13]. Local charts are used to describe the differential manifold, with compatibility conditions on the intersection of the open sets (atlases) covering the manifold. For example, the crucial issue of constructing manifold splines in [10, 11] is obtaining an affine structure of a manifold, i.e. a set of equivalent affine atlases. By these affine atlases, one can define splines on a manifold (a physical domain) based on classical splines defined on a rectangular parametric domain, such as triangular B-spline based manifold splines [10] and T-spline based manifold splines [11]. Because these splines are well defined on the intersection of affine atlases.

Different from manifold splines, splines defined on a mesh, such as [14], are defined on a parametric domain (a mesh). By generalising the topology of a mesh, splines defined on meshes with more general topologies can be used to describe a complex geometry globally. In the framework of Isogeometric analysis, splines defined on a parametric mesh are used to describe a geometry (a physical domain), called generating a parameterization. By this parameterization, a PDE is pulled back to the parametric domain and solved on the parametric domain by the same splines, such as NURBS-based Isogeometric analysis [3]. In this paper, we propose of splines on rectangular meshes with arbitrary topology and analyze the property of these splines for applying them to solving PDEs in the framework of isogeometric analysis without decomposing the structured meshes.

The structure of this paper is summarised. From Section 2 to Section 3, we focus on defining this type of spline spaces, the dimension formulae and basis construction for a bicubic spline space with C^1 parameter continuity. The basis functions are called Hermite bases. Based on Hermite bases, from Section 4 to Section 5, the property of Hermite bases is discussed for solving PDEs over a complex physical domain in the framework of Isogeometric analysis, such as requirements for parameterizations and C^1 -test functions on a physical domain in Section 4, the interpolation approximation error in Section 5.1 and the numerical convergence rate in Section 5.2. The last section proposes a conclusion of our work and directions for future works.

2. Meshes in the parametric plane and spline spaces

In this section, the fundamental definitions of this paper will be presented. First, in Section 2.1, the concept of parametric meshes is given. Its definition includes an equivalence relation, which allows to address general topologies. Then the definition of spline spaces over a parametric mesh is introduced in Section 2.2.

2.1. Parametric meshes

In this section, we introduce our concept of a parametric mesh, which generalizes the notion of a mesh in the parametric space, considered, e.g., in [17], [8] and [14]. Concretely, in Section 2.1.1, the definition of parametric meshes is given. Then, some concepts are introduced in Section 2.1.2, such as local frames, hanging vertices, basis vertices and composite edges of a parametric mesh, which is used in Sections 2.2 and 3. Moreover, the local refinement of meshes is used in adaptive finite element method. Section 2.1.3 introduces how to perform a local refinement of a parametric mesh. In the process, the definition of hierarchical parametric meshes is presented based on a local refinement process.

2.1.1. Definition of Parametric Meshes

Notation 2.1. *The metric plane \mathbb{R}^2 equipped with coordinates (s, t) , will be called the (s, t) -plane. A cell is a rectangle of \mathbb{R}^2 . We will use the letter C with indices to denote cells. The boundary of a cell is decomposed into a finite set of segments (at least 4 but maybe more), called the edges of the cell. We will use the letter e with indices to denote edges. The end points of these edges are called the vertices of the cell. We will use the letters v or w with indices to denote vertices. In other words, edges are segments between adjacent vertices.*

We will consider an equivalence relation on the vertices (resp. edges) of a union of cells. Before providing a formal definition of our concept, let us illustrate it with a simple example to show a parametric mesh with arbitrary topology.

Example 2.1 (A parametric mesh with arbitrary topology). *The left mesh of Figure 3 shows a parametric mesh \mathcal{M} . Its equivalent vertices have been marked with the same vertex labels and the edges between equivalent vertices are equivalent.*

The topological structure of \mathcal{M} is the same as the topology of a “usual” mesh, shown on the right side of Figure 3. From this example, a parametric mesh allows extraordinary vertices, whose valences are not 4.

Now, the formal definition of a parametric mesh is presented.

Definition 2.1 (Parametric Mesh). *A parametric mesh \mathcal{M} is given by a collection of cells denoted by C_1, C_2, \dots, C_N , a subset \mathcal{P}_F of $\mathbf{I} = \{\{i, j\} : i, j \in \{1, 2, \dots, N\} \text{ and } i \neq j\}$, a collection of transition maps indexed by \mathcal{P}_F , and an equivalence relation “ \sim ” on the edges and vertices of the cells, satisfying the following properties.*

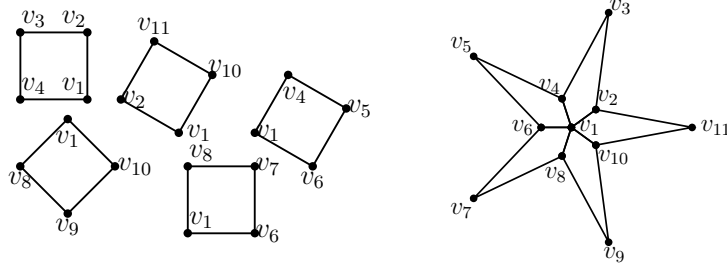


Figure 3: A parametric mesh \mathcal{M} with 5 cells (left) and a “usual” mesh with the same topology of \mathcal{M}

1. For each pair $(i, j) \in \mathcal{P}_F$, there exists a pair of transition maps:

- $\phi_{i,j} : C_i \rightarrow \mathbb{R}^2$,
- $\phi_{j,i} : C_j \rightarrow \mathbb{R}^2$

and a pair of edges $e_{i,j}$ of C_i and $e_{j,i}$ of C_j such that

- $\phi_{i,j}(C_i) \cap C_j = e_{j,i}$,
- $\phi_{j,i}(C_j) \cap C_i = e_{i,j}$,
- $\phi_{i,j}|_{e_{i,j}} : e_{i,j} \rightarrow e_{j,i}$, $\phi_{j,i}|_{e_{j,i}} : e_{j,i} \rightarrow e_{i,j}$ are diffeomorphisms and $(\phi_{i,j}|_{e_{i,j}})^{-1} = \phi_{j,i}|_{e_{j,i}}$.

Then, $e_{i,j} \sim e_{j,i}$.

Moreover, for any two vertices v of $e_{i,j}$ and w of $e_{j,i}$, if $\phi_{i,j}(v) = w$ then $v \sim w$.

2. For any edge e of C_i ($i = 1, 2, \dots, n$), the number of edges that are equivalent to e by “ \sim ” is no more than 2.

Definition 2.2 (Interior vs Boundary, degree). The equivalence class of edges and vertices of C_i are called \mathcal{M} ’s edges and vertices. If an edge equivalence class has two elements, then it is called an interior edge of \mathcal{M} ; otherwise it is called a boundary edge. If a vertex is on a boundary edge, then it is called a boundary vertex; otherwise, it is called an interior vertex. The degree $\deg(v)$ of an equivalence class of vertices v is the number of distinct equivalence classes of edges e containing v .

Example 2.2. In Example 2.1, note that, e.g., v_6v_7 is a boundary edge, while v_1v_2 and v_1v_6 are interior edges (because they are shared by two cells). We have $\deg(v_1) = 5$, $\deg(v_2) = 3$ and $\deg(v_3) = 2$.

Remark 2.2 (Restrictions).

- A parametric mesh can also describe a non-orientable surface, such as the Moebius strip. However, in this article, we will restrict ourselves to the case where \mathcal{M} is orientable. Furthermore, we suppose that any edge (resp. vertex) of a cell is not equivalent to another edge (resp. vertex) of the same cell.

2.1.2. *Local frames, hanging vertices, basis vertices and composite edges of a parametric mesh*

Let \mathcal{M} be a parametric mesh and denote its cells as C_1, C_2, \dots, C_N . For each cell $C_i, i = 1 \dots N$, we define a local frame by two unit vectors $\mathcal{F}_i := (\mathbf{s}_i, \mathbf{t}_i)$ that parallel each of the two directions of the edges of C_i (and that agrees with the metric of the (s, t) -plane). This is illustrated in Figure 4.

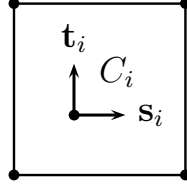


Figure 4: A local frame of C_i

Now consider two adjacent cells C_1 and C_2 of \mathcal{M} , (i.e., that share a common edge).

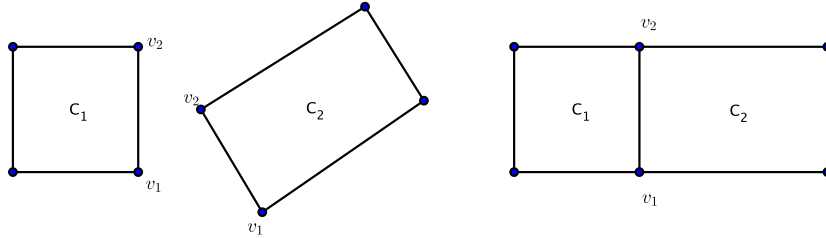


Figure 5: Transition maps

They can be moved together by the transition map, which is a rigid transformation. This is illustrated in Figure 5. By this way, \mathcal{M} becomes another parameter mesh \mathcal{M}' with identity transition maps between two adjacent cells, where \mathcal{M}' is called an equivalent parametric mesh of \mathcal{M} .

Example 2.3 (A T-mesh). *A planar T-mesh, as defined in [17], can be represented by a parametric mesh such as the right side of Figure 6, where all of the transition maps are identity maps.*

In the left side of Figure 6 there is another parametric mesh with all of the transition maps, which are rigid transformations. The T-mesh in the right side of Figure 6 is an equivalent parametric mesh of the parametric mesh in the left side of Figure 6.

Definition 2.3. *Here, we present the definitions of a hanging vertex, basis vertex and composite edge.*

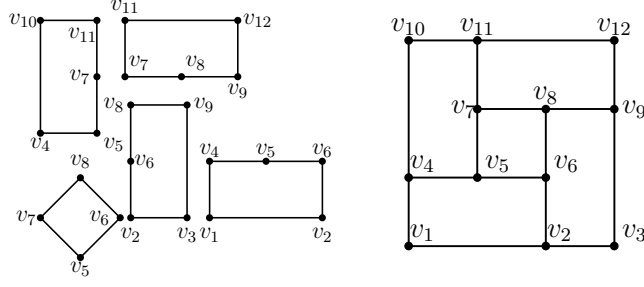


Figure 6: A parametric mesh with rigid transformations and its equivalent parametric mesh with identity transition maps

- An interior vertex v of \mathcal{M} is called a *hanging vertex* if there is a cell C such that v is on an edge of C and it is not a corner point of C .
- A vertex of \mathcal{M} that is not a hanging vertex is called a *basis vertex*.
- A *composite edge* of \mathcal{M} is the longest possible “line segment” that consists of several interior edges, and each non-end vertex of this “line segment” is a hanging vertex of \mathcal{M} , where if two edges locate on the same line or not, this point is determined by their positions in \mathcal{M} ’s equivalent parametric mesh.

Example 2.4. In the left side of Figures 6, the vertices v_5, v_7, v_6 and v_8 are hanging vertices. v_9 is not a hanging vertex. Because it is a boundary vertex and it is a corner point of a cell. v_5v_7 is an interior edge, and v_5v_{11} is a composite edge that includes two edges v_5v_7 and v_7v_{11} . Because v_5v_{11} lies on the same line of its equivalent parametric mesh (T -mesh), shown in the right side of Figure 6, it satisfies the definition of “a composite edge”.

Remark 2.3. If \mathcal{M} has no hanging vertices and all of its cells are unit squares, it is a **spline domain**, as defined in [14].

2.1.3. Local Refinement and Hierarchical parametric meshes

In adaptive finite element analysis, refinement is an important operation. Traditionally, one distinguishes between two types of refinement: h-refinement and p-refinement. The first one, also called h-adaptivity, amounts to splitting elements in space while keeping their polynomial degree fixed, whereas p-adaptivity amounts to increasing the polynomial degrees.

Hereafter, a simple scheme of the local h-refinement of \mathcal{M} is presented. The refinement does not change the topology of \mathcal{M} .

Definition 2.4 (Local Refinement Rule). Let \mathcal{M} be a parametric mesh. A refined parametric mesh \mathcal{M}' is obtained by splitting some of the cells of \mathcal{M} along lines parallel to one of the edges of these cells. The transition maps of \mathcal{M}' are defined as follows.

- Given two cells C_i and C_j of \mathcal{M} with an adjacent edge $e_{i,j} \sim e_{j,i}$ which is split, for any cells $C'_i \subset C_i$, $C'_j \subset C_j$ of \mathcal{M}' with a common sub-edge of $e_{i,j} \sim e_{j,i}$, the transition map between C'_i and C'_j is the restriction respectively to C'_i and C'_j of the transition maps $\phi_{i,j} : C_i \rightarrow \mathbb{R}^2$ and $\phi_{j,i} : C_j \rightarrow \mathbb{R}^2$.
- For a cell C of \mathcal{M} split into sub-cells C'_1, C'_2 of \mathcal{M}' along an edge e' , the transition map across e' is the identity.

This refinement construction can be iterated. Notice that the refinements create additional hanging vertices.

Definition 2.5 (Hierarchical parametric mesh). A hierarchical parametric mesh \mathcal{M} is a mesh obtained by the iterated refinement of an initial parametric mesh, where we will also assume that the initial mesh has no hanging vertex.

If the initial mesh is just a cell, \mathcal{M} is a hierarchical T-subdivision, as described in [25].

2.2. Spline spaces over a parametric mesh

In this section, based on the definition of a parametric mesh in Section 2.1, we define the spline space over a parametric mesh in Section 2.2.1. Formally, this definition depends on the choice of local frames. In Section 2.2.2, the local frame independency is checked. After that, in Section 2.2.3, the nesting property of spline spaces is presented by the local refinement of parametric meshes. This property is usually required in adaptive finite element analysis.

2.2.1. Definition of spline spaces over a parametric mesh

Definition 2.6 (Spline over \mathcal{M}). A spline f of bi-degree (d, d) and C^r regularity over \mathcal{M} with the local frame set $\mathcal{F} = \{\mathcal{F}_i\}$ is given by a collection of polynomials f_i satisfying

1. $f_i(s_i, t_i) := f|_{C_i} \in \mathbb{R}_{d,d}[s_i, t_i]$, $i = 1 \dots N$, where (s_i, t_i) is the coordinates associated with the given local frame \mathcal{F}_i of C_i ;
2. If $v_{i,j} \sim v_{j,i}$ is a (class) of vertex common to cells C_i and C_j of \mathcal{M} , then

$$f_i(v_{i,j}) = f_j(v_{j,i}).$$

3. If $e_{i,j} \sim e_{j,i}$ is a (class) of edge common to cells C_i and C_j of \mathcal{M} , then $f_i(s_i, t_i)$ and $f_j(s_j, t_j)$ are “ C^r across the edge” (we will also say that they have a C^r fit).

More precisely, let $\phi_{i,j}, \phi_{j,i}$ be the transition maps between C_i and C_j , such that $\phi_{i,j}(e_{i,j}) = e_{j,i}$; denote as $\mathbf{n}_{i,j}$ and $\mathbf{n}_{j,i}$ unit vectors of the metric (s, t) -plane, perpendicular, respectively, to $e_{i,j}$ and $e_{j,i}$. Then, we must have

$$D_{\mathbf{n}_{i,j}}^k (f_j \circ \phi_{j,i}^{-1})|_{e_{i,j}} = D_{\mathbf{n}_{i,j}}^k f_j|_{e_{i,j}} \quad (1)$$

$$D_{\mathbf{n}_{j,i}}^k (f_i \circ \phi_{i,j}^{-1})|_{e_{j,i}} = D_{\mathbf{n}_{j,i}}^k f_i|_{e_{j,i}} \quad (2)$$

for $k = 0, 1, 2, \dots, r$.

Remark 2.4. If $\forall \phi_{i,j}, \phi_{j,i}$ are rigid transformations and $\forall C_i$ are unit squares, then the splines defined here are C^r -splines in [14].

Notation 2.5. We denote by $\mathbf{S}(d, r; \mathcal{M})$ the set of splines defined in Definition 2.6. We call it a spline space over \mathcal{M} .

We have:

- By linearity of directional derivatives, $\mathbf{S}(d, r; \mathcal{M})$ is a vector space;
- It is finite dimensional;
- $1 \in \mathbf{S}(d, r; \mathcal{M})$.

Remark 2.6. For rigid transformations maps that are C^k -diffeomorphisms, conditions (1) and (2) are equivalent.

2.2.2. Spline space and local frames

Let us discuss the dependency of the spline space \mathcal{M} on the choice of local frames \mathcal{F}_i for the cells C_i .

Considering another local frame \mathcal{F}'_i , there exists a set of orthogonal transformations $\mathbf{O} = \{\mathbf{O}_i\}$ such that

$$\mathcal{F}_i = \mathbf{O}_i \mathcal{F}'_i, i = 1 \dots N.$$

By the action of \mathbf{O}_i , any polynomial in the coordinates of \mathcal{F}_i becomes a polynomial in the coordinates of \mathcal{F}'_i of the same degree. Moreover, the other two items in Definition 2.6, evaluation at a vertex and regularity, are conserved when expressed in the other frame. This proves the following theorem.

Theorem 2.7 (\mathcal{F} Independency). Let \mathcal{F} and \mathcal{F}' be two local frames of \mathcal{M} . Then, for each cell C_i , $i = 1 \dots N$, of \mathcal{M} , there exists an orthogonal transformation \mathbf{O}_i sending \mathcal{F}'_i to \mathcal{F}_i , i. e., $\mathcal{F}_i = \mathbf{O}_i \mathcal{F}'_i$. If $f \in \mathbf{S}(d, r; \langle \mathcal{M}, \mathcal{F} \rangle)$, so that

$$f \circ \mathbf{O} \in \mathbf{S}(d, r; \langle \mathcal{M}, \mathcal{F}' \rangle),$$

where $\mathbf{O}|_{\mathcal{F}_i} = \mathbf{O}_i$, $f \circ \mathbf{O}|_{C_i} = f(\mathbf{O}_i(s'_i, t'_i))$, where $\mathbf{S}(d, r; \langle \mathcal{M}, \mathcal{F} \rangle)$ is a spline space over \mathcal{M} with the local frames \mathcal{F} . Its bi-degree is (d, d) and, it has C^r regularity.

Thus, up to a set of orthogonal transformations, splines over \mathcal{M} are independent of the choice of \mathcal{F} .

2.2.3. Local refinement and spline spaces

Let \mathcal{M}' be a parametric mesh obtained by refining some cells of \mathcal{M} . Then, a spline function in $\mathbf{S}(d, r; \mathcal{M})$ is a spline function defined over the refined mesh \mathcal{M}' , owing to the local refinement rule in Definition 2.4.

Thus, we have the nesting property:

$$\mathbf{S}(d, r; \mathcal{M}) \subseteq \mathbf{S}(d, r; \mathcal{M}').$$

In particular, we still have $1 \in \mathbf{S}(d, r; \mathcal{M}')$.

3. Bicubic spline spaces over a parametric mesh

In this section, bicubic spline spaces over a parametric mesh will be considered. We also consider transition maps that are rigid transformations of the plane. The main results in this section present the dimension formula and a set of bases, where Hermite data play a crucial role.

Let \mathcal{M} be a hierarchical mesh. The bicubic spline spaces over \mathcal{M} is $\mathbf{S}(3, 1; \mathcal{M})$. Here, we organize this section as follows. In Section 3.1, the Hermite data of a bicubic spline over a parametric mesh are discussed. Based on the analysis of Section 3.1, in Section 3.2, the dimension formula of $\mathbf{S}(3, 1; \mathcal{M})$ and a set of bases are presented.

3.1. Hermite data

In this section, a linear map \mathcal{H} is introduced. By \mathcal{H} , a spline in $\mathbf{S}(3, 1; \mathcal{M})$ is described by its Hermite data at each vertex of \mathcal{M} . Then, the constraints between its Hermite data are given, such that the constraints across a common edge (Section 3.1.1) become the constraints of the Hermite data at a basis vertex and hanging vertex (Section 3.1.2). By these constraints, \mathcal{H} is reduced to a new injective map $\widetilde{\mathcal{H}}$.

We first illustrate the Hermite data construction on a single square. Let Q be the square in the parametric (s, t) -plane with vertices $v_1 := [0, 0]$, $v_2 := [0, 1]$, $v_3 := [1, 0]$, and $v_4 := [1, 1]$. The vector space E of polynomials of bidegree $(3, 3)$ on Q has dimension 16 and a basis of E is formed by the two by two products of Bernstein polynomials $B_i^3(s)$ and $B_j^3(t)$ for $0 \leq i, j \leq 3$.

We set

$$H_{(s,t)}^{v_\ell}(f) = (f(v_\ell), \frac{\partial f}{\partial s}(v_\ell), \frac{\partial f}{\partial t}(v_\ell), \frac{\partial^2 f}{\partial s \partial t}(v_\ell))$$

for $1 \leq \ell \leq 4$.

The 4 Hermite data $H_{(s_i, t_i)}^{v_\ell}(f)$ at each of the 4 vertices form 16 real numbers naturally associated with an element f of E .

Lemma 3.1. *The linear map $E \longrightarrow \mathbb{R}^{16}$ defined by the Hermite data at the 4 vertices of Q is an isomorphism.*

Proof. It suffices to check the non vanishing of the determinant of the corresponding matrix on the basis $B_i^3(s)B_j^3(t)$, $0 \leq i, j \leq 3$. \square

Notice that $H^{v_\ell}(f)$ depends only on the four Bernstein coefficients that are near v_ℓ as in the B-net method described in [17]. By this correspondence, the dimension formula and basis construction of $\mathbf{S}(3, 1; \mathcal{M})$ are discussed by generalizing the B-net method in [17].

Let \mathcal{M} 's cells be C_1, \dots, C_N . We extend the definition of the Hermite data to the spline space $\mathbf{S}(3, 1; \mathcal{M})$ and via the following map:

$$\begin{aligned} \mathcal{H} : \mathbf{S}(3, 1; \mathcal{M}) &\rightarrow \mathbb{R}^{4N} \\ f &\mapsto (H_{(s_i, t_i)}^{v_\ell}^i(f_i))_{i=1, \dots, N, \ell=1, \dots, 4} \end{aligned} \quad (3)$$

where $v_\ell^i, \ell = 1, \dots, 4$ are the 4 vertices of cell C_i and $H_{(s_i, t_i)}^{v_\ell^i}(f_i)$ are the Hermite data of f at v_ℓ^i .

Lemma 3.2. *The Hermite data map \mathcal{H} defined in (3) is an injective linear map from $\mathbf{S}(3, 1; \mathcal{M})$ to \mathbb{R}^{4N} .*

Proof. By construction, \mathcal{H} is linear. To prove that it is injective, we note that if all Hermite data of a polynomial f_i at the vertices of a cell C_i are zero, then by Lemma 3.1, $f_i \equiv 0$. Thus, if $f \in \mathbf{S}(3, 1; \mathcal{M})$ is such that $\mathcal{H}(f) = 0$ then $f = 0$. \square

We now analyze different constraints applicable on the Hermite data at a vertex of \mathcal{M} .

3.1.1. Hermite data across a common edge

In this section, we describe a C^1 regularity condition across an edge in terms of Hermite data.

Lemma 3.3. *Let C_1, C_2 be two cells with the common edge $e_{1,2} = v_1 v_2$. Assume that they share the same local frame (\mathbf{s}, \mathbf{t}) and the same parameters (s, t) . Then $f_1(s, t)$ and $f_2(s, t)$ are C^1 across $e_{1,2}$ if and only if their Hermite data at v_1 and v_2 coincide:*

$$H_{(s,t)}^{v_\ell}(f_1) = H_{(s,t)}^{v_\ell}(f_2), \quad l = 1, 2.$$

Proof. Suppose that the edge $e_{1,2}$ is along the t -direction (the other case can be treated symmetrically). Because $f_1(s, t)$ and $f_2(s, t)$ are polynomials of bi-degree $(3, 3)$, if their Hermite data coincide at v_1 and v_2 , then we have $f_1(s, t) = f_2(s, t)$ and $\partial_s f_1(s, t) = \partial_s f_2(s, t)$ along the edge $v_1 v_2 = e_{1,2}$. In other words, the function defined by (f_1, f_2) is C^1 across the edge $e_{1,2}$.

Conversely, if (f_1, f_2) is C^1 across the edge $e_{1,2}$, then their Hermite data at v_1 and v_2 must coincide. \square

Assume now that C_1 and C_2 have different frames, denoted by $\mathcal{F}_1 = (\mathbf{s}_1, \mathbf{t}_1)^T$ and $\mathcal{F}_2 = (\mathbf{s}_2, \mathbf{t}_2)^T$. There must exist an orthogonal transformation $\mathbf{O}_{2,1}$, more precisely a rotation of angle $k\pi/2$ ($k \in \mathbb{Z}$), such that

$$\mathcal{F}_2 = \mathbf{O}_{2,1} \mathcal{F}_1, \quad \mathbf{O}_{2,1} = \begin{pmatrix} O_{11} & O_{12} \\ O_{21} & O_{22} \end{pmatrix}. \quad (4)$$

The following lemma describes the relations between $H_{(s_1, t_1)}^{v_\ell}(f_1)$ and $H_{(s_2, t_2)}^{v_\ell}(f_2)$.

Lemma 3.4. *$f_1(s_1, t_1)$ and $f_2(s_2, t_2)$ have a C^1 fit if and only if*

$$H_{(s_2, t_2)}^{v_\ell}(f_2)^T = A H_{(s_1, t_1)}^{v_\ell}(f_1)^T, \quad (5)$$

where

$$A = \begin{pmatrix} 1 & 0 & 0 & 0 \\ 0 & O_{11} & O_{12} & 0 \\ 0 & O_{21} & O_{22} & 0 \\ 0 & 0 & 0 & O_{11}O_{22} + O_{12}O_{21} \end{pmatrix} \quad (6)$$

where $O_{i,j}$ ($i, j = 1, 2$) are defined in (4).

Proof. By Lemma 3.3, after applying the transition map, we have $H_{(s_1, t_1)}^{v_\ell}(f_1)^T = H_{(s_2, t_2)}^{v_\ell}(f_2)^T$. Thus, we just considered the Hermite data at v_ℓ of f_2 using different frames $\mathcal{F}_1, \mathcal{F}_2$. Based on the fact that $\mathbf{O}_{2,1}$ in (4) is an orthogonal rotation of angle $k\pi/2$, we explicitly computed matrix A and obtained formula (6). \square

Remark 3.5. Because $\mathbf{O}_{2,1}$ in (4) is a rotation of angle $k\pi/2$, we have $O_{11}O_{22} + O_{12}O_{21} = (-1)^k$; consequently $\text{rank}(A) = 4$.

This shows that the Hermite data at v_ℓ on C_2 is uniquely determined by the Hermite data at v_ℓ on C_1 , via the linear invertible transformation A . In this case we will say that the Hermite data at v_ℓ on C_1 and C_2 are **compatible**.

3.1.2. Hermite data at a basis vertex of degree n and a hanging vertex

Let v be a basis vertex of \mathcal{M} and n be the degree of v . This means that there are n cells C_1, \dots, C_n with v as one of their corner vertices. These cells form v 's 1-neighborhood. Let us consider the behavior of $f \in \mathbf{S}(3, 1; \mathcal{M})$ at v .

We can assume that we have already sorted the 1-neighborhood of v such that two successive cells share a common edge of \mathcal{M} in a clockwise direction.

Given a local frame $\mathcal{F}_1 = (\mathbf{s}_1, \mathbf{t}_1)^T$ of C_1 , the local frame \mathcal{F}_k of C_k is defined as

$$\mathcal{F}_k = \mathbf{O}_{k,1} \mathcal{F}_1, \quad (7)$$

where

$$\mathbf{O}_{k,1} = \begin{pmatrix} \cos(\pi(k-1)/2) & -\sin(\pi(k-1)/2) \\ \sin(\pi(k-1)/2) & \cos(\pi(k-1)/2) \end{pmatrix}$$

According to C^1 continuity, the Hermite data at v of C_k is obtained by Eq. (4) and Eq. (5), i.e.,

$$H_{(s_k, t_k)}^v(f_k)^T = A_k H_{(s_1, t_1)}^v(f_1)^T, \quad (8)$$

where $f_i = f|_{C_i}$, A_k is determined by $\mathbf{O}_{k,1}$, similarly to Eq. (5). Because v is a basis vertex, it can be a boundary vertex as well as an interior (not hanging) vertex. If v is a boundary vertex of \mathcal{M} , the Hermite data of $H_{(s_k, t_k)}^v(f)$ ($k > 1$) are well determined when $H_{(s_1, t_1)}^v(f)$ is given because $\text{rank}(A_k) = 4$.

Proposition 3.6. *With the previous notations, if v is an interior basis vertex and n is its degree, we have*

1. If $n \bmod 4 = 1$, then,

$$\frac{\partial f(v)}{\partial s_1} = 0, \quad \frac{\partial f(v)}{\partial t_1} = 0, \quad \frac{\partial^2 f(v)}{\partial s_1 \partial t_1} = 0;$$

2. If $n \bmod 4 = 2$, then

$$\frac{\partial f(v)}{\partial s_1} = 0, \quad \frac{\partial f(v)}{\partial t_1} = 0;$$

3. If $n \bmod 4 = 3$, then

$$\frac{\partial f(v)}{\partial s_1} = 0, \quad \frac{\partial f(v)}{\partial t_1} = 0, \quad \frac{\partial^2 f(v)}{\partial s_1 \partial t_1} = 0.$$

Proof.

If v is an interior vertex of \mathcal{M} and its degree is n . Consider C_1 and C_n stick together clockwise, by (8),

$$H_{(s_n, t_n)}^v(f_n)^T = A_n H_{(s_1, t_1)}^v(f_1)^T, \quad (9)$$

where $H_{(s_i, t_i)}^v(f_j)$ is the Hermite data at v on C_j with respect to the local frame $(\mathbf{s}_i, \mathbf{t}_i)$, $f_j = f|_{C_j}$, A_n is defined in (8).

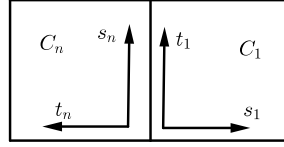


Figure 7: C_1 and C_n stick anticlockwise

Considering C_1 and C_n stick together anticlockwise, the common edge is along \mathbf{t}_1 of C_1 and \mathbf{s}_n of C_n (shown in Figure 7). Then

$$\begin{pmatrix} \mathbf{s}_1 \\ \mathbf{t}_1 \end{pmatrix} = \begin{pmatrix} 0 & -1 \\ 1 & 0 \end{pmatrix} \begin{pmatrix} \mathbf{s}_n \\ \mathbf{t}_n \end{pmatrix}$$

Thus, $H_{(s_1, t_1)}^v(f_n)^T = B H_{(s_n, t_n)}^v(f_n)^T$ and by (9),

$$H_{(s_1, t_1)}^v(f_n)^T = B A_n H_{(s_1, t_1)}^v(f_1)^T,$$

where $B = \begin{pmatrix} 1 & 0 & 0 & 0 \\ 0 & 0 & -1 & 0 \\ 0 & 1 & 0 & 0 \\ 0 & 0 & 0 & -1 \end{pmatrix}.$

f_1 and f_n are C^1 across the common edge with v as their common vertex. By Lemma 3.3, $H_{(s_1, t_1)}^v(f_n) = H_{(s_1, t_1)}^v(f_1)$, i.e.,

$$B A_n H_{(s_1, t_1)}^v(f_1)^T = H_{(s_1, t_1)}^v(f_1)^T.$$

Thus $(I - BA_n)H_{(s_1, t_1)}^v(f_1)^T = 0$.

$$\text{When } n \bmod 4 = 1, I - BA_n = \begin{pmatrix} 0 & 0 & 0 & 0 \\ 0 & 1 & 1 & 0 \\ 0 & -1 & 1 & 0 \\ 0 & 0 & 0 & 2 \end{pmatrix};$$

$$\text{when } n \bmod 4 = 2, I - BA_n = \begin{pmatrix} 0 & 0 & 0 & 0 \\ 0 & 2 & 0 & 0 \\ 0 & 0 & 2 & 0 \\ 0 & 0 & 0 & 0 \end{pmatrix};$$

$$\text{when } n \bmod 4 = 3, I - BA_n = \begin{pmatrix} 0 & 0 & 0 & 0 \\ 0 & 1 & -1 & 0 \\ 0 & 1 & 1 & 0 \\ 0 & 0 & 0 & 2 \end{pmatrix}.$$

The result of this proposition is obtained. \square

We recall that, by Definition 2.3, a hanging vertex v is a non end vertex of a composite edge, which belongs to the interior of a segment joining two corner points of a cell. For hanging vertices, similar to Theorem 4.2 in [17], we get

Lemma 3.7. *Let v_0, v_1, \dots, v_ℓ be all vertices on a composite edge of \mathcal{M} and $f \in \mathbf{S}(3, 1; \mathcal{M})$. Then the Hermite data $H^{v_i}(f)$ depends linearly on $H^{v_0}(f)$ and $H^{v_\ell}(f)$, where v_i is a hanging vertex, for $i = 1, 2, \dots, \ell - 1$.*

Moreover, a hierarchical parametric mesh is T-cycle free. For a T-cycle free mesh, the Hermite data at a hanging vertex can be decided by the Hermite data at basis vertices, as [18].

Let \mathcal{M} be a hierarchical mesh. The results of Sections 3.1.1, and 3.1.2 imply the following proposition.

Proposition 3.8. *The map \mathcal{H} defined in (3) can be reduced to*

$$\begin{aligned} \widetilde{\mathcal{H}} : \mathbf{S}(3, 1; \mathcal{M}) &\rightarrow \mathbb{R}^{4N_1 + 2N_2 + N_3}, \\ f &\mapsto \bigoplus_{v \in V} \widetilde{H}^v(f) \end{aligned}$$

where V is the set of basis vertices of \mathcal{M} and

- $\widetilde{H}^v(f) = H^v(f)$, if v is a boundary vertex or $\deg(v) \bmod 4 = 0$,
- $\widetilde{H}^v(f) = [f(v), \frac{\partial^2 f(v)}{\partial s \partial t}]$, if $\deg(v) \bmod 4 = 2$,
- $\widetilde{H}^v(f) = [f(v)]$, if $\deg(v) \bmod 2 = 1$.

Here, N_1 is the number of boundary vertices and interior basis vertices with $\deg(v) \bmod 4 = 0$, N_2 is the number of interior basis vertices with $\deg(v) \bmod 4 = 2$, and N_3 is the number of interior basis vertices with $\deg(v) \bmod 2 = 1$. $\widetilde{\mathcal{H}}$ is injective.

Indeed, based on Lemma 3.7, if all Hermite data at the basis vertices vanish, then $H^v(f) = \mathbf{0}$ for any vertex v of \mathcal{M} . Thus, for any cell of \mathcal{M} , the Hermite data of f at any vertex of this cell is zero, i.e., $f \equiv 0$. In other words, $\widetilde{\mathcal{H}}$ is injective.

In the next section, we will construct splines associated with a basis vertex of a hierarchical parametric mesh \mathcal{M} and prove that \mathcal{H} is surjective.

3.2. Dimension formulas and Hermite bases

In this section, \mathcal{M} is a hierarchical parametric mesh obtained by a sequence of refinements:

$$\mathcal{M}^0 \longrightarrow \dots \mathcal{M}^k \longrightarrow \dots \longrightarrow \mathcal{M}^l = \mathcal{M}.$$

We will continue to analyze $\widetilde{\mathcal{H}}$ introduced in Proposition 3.8. By proving that $\widetilde{\mathcal{H}}$ is a surjection, the dimension formulae of $\mathbf{S}(3, 1; \mathcal{M})$ are given, and the spline set constructed in Theorem 3.10 is a basis set called Hermite bases.

As we have seen (Proposition 3.8), a spline function f over \mathcal{M} is uniquely determined by its Hermite data $\widetilde{\mathcal{H}}(f)$. The following lemma shows that the image of the linear map $\widetilde{\mathcal{H}}$ is the vector space of Hermite data that are compatible across each edge of \mathcal{M} .

Lemma 3.9. *If the Hermite data at the vertices of the cells C_1, \dots, C_N are compatible, there exists a unique element $f \in \mathbf{S}(3, 1; \mathcal{M})$ with this Hermite data.*

Proof. Let us consider two vertices v_1, v_2 of a common edge between two cells C_{i_1}, C_{i_2} of \mathcal{M} . We can assume that the transition map is the identity map. Let f_1 (resp. f_2) be the unique function constructed from the Hermite data at the vertices on C_1 (resp. C_2). By Lemma 3.3, f_1 and f_2 are C^1 across the common edge (v_1, v_2) . This shows that the piecewise polynomial function f constructed on each cell C_1, \dots, C_N of \mathcal{M} from the Hermite data at their vertices is in $\mathbf{S}(3, 1; \mathcal{M})$. As $\widetilde{\mathcal{H}}$ is injective, the function f is uniquely determined by its Hermite data. \square

In the following, we are going to construct linearly independent spline functions in $\mathbf{S}(3, 1; \mathcal{M})$. This set of spline functions is a basis of $\mathbf{S}(3, 1; \mathcal{M})$.

To construct this basis, we proceed as follows. We will associate $J = 1, 2$ or 4 splines f_v^j with each basis vertex v of \mathcal{M} ; the choice of J follows a rule described in the theorem below. We do not associate splines with hanging vertices.

Theorem 3.10. *Let v be any basis vertex of a hierarchical parametric mesh \mathcal{M} . We can associate with v a family of J splines f_v^j , $j = 1 \dots J$, (J is indicated below), such that the Hermite data of each f_v^j , $j = 1 \dots J$ at all other basis vertices $w \neq v$ of \mathcal{M} are 0. While J and the Hermite data of each f_v^j , $j = 1 \dots J$ at v are as follows.*

1. *If v is a boundary vertex or an interior vertex with $\deg(v) \bmod 4 = 0$, then $J = 4$ and the Hermite data can be set equal to any one of the following choices:*

$$[1, 0, 0, 0], [0, 1, 0, 0], [0, 0, 1, 0], [0, 0, 0, 1].$$

2. If v is an interior vertex and $\deg(v) \bmod 2 = 1, 3$, then $J = 1$, and the Hermite data can be set equal to $[1, 0, 0, 0]$.
3. If v is an interior vertex and $\deg(v) \bmod 4 = 2$, then $J = 2$ and the Hermite data can be set equal to any one of the following choices:

$$[1, 0, 0, 0], [0, 0, 0, 1].$$

Proof.

Let us first compute the Hermite data for all of the vertices of the cells of \mathcal{M} .

1. Set the Hermite data for all basis vertices $w \neq v$ to zero. They naturally satisfy the constraints described in Section 3.1. Thus they are compatible.
2. Set the Hermite data at v to any of the vectors mentioned in this theorem. By the constraint analysis of Section 3.1, they satisfy the compatibility condition.
3. For the Hermite data at a hanging vertex, they can be decided by the Hermite data at basis vertices of \mathcal{M} as analysing after Lemma 3.7.

By Lemma 3.9, there exists a unique element of $\mathbf{S}(3, 1; \mathcal{M})$ corresponding to these Hermite data. It satisfies the requirement of this theorem. \square

A direct consequence of this result is the following:

Corollary 3.11. $\widetilde{\mathcal{H}}$ is surjective.

We deduce the dimension formula for $\mathbf{S}(3, 1; \mathcal{M})$.

Theorem 3.12 (Dimension formula). Let \mathcal{M} be a hierarchical parametric mesh.

$$\dim \mathbf{S}(3, 1; \mathcal{M}) = 4N_1 + 2N_2 + N_3,$$

where N_1 is the number of boundary vertices and interior basis vertices with $\deg(v) \bmod 4 = 0$, N_2 is the number of interior basis vertices with $\deg(v) \bmod 4 = 2$, and N_3 is the number of interior basis vertices with $\deg(v) \bmod 4 = 1, 3$.

Remark 3.13. For $\mathbf{S}(d, r, \mathcal{M})$, we can analyze its dimension formula with the same method presented for $\mathbf{S}(3, 1, \mathcal{M})$, where $d = 2r + 1$.

Using the functions defined by Theorem 3.10, we get a set of bases of $\mathbf{S}(3, 1; \mathcal{M})$ called the **Hermite bases** of $\mathbf{S}(3, 1; \mathcal{M})$. In particular, we have the following property:

Corollary 3.14 (Local Support). Assume that \mathcal{M} has no hanging vertices. Let $f_{v_i}^1, f_{v_i}^2, \dots, f_{v_i}^{n_i}$ be all of the splines associated with the vertex v_i . Then, the support of each $f_{v_i}^j$ is within the 1-neighborhood of v_i .

Proof. If the mesh has no hanging vertices, the Hermite data of the basis functions in Theorem 3.10 associated with a vertex v vanish at all other vertices $w \neq v$. Thus, their supports are in the union of cells of \mathcal{M} containing v . \square

Remark 3.15. *The spline functions that we consider are C^1 -functions, after a local rigid transformation of the coordinate systems of a cell. This property is connected to the notion of geometry continuity or G^1 continuity for surfaces, where a continuity of the tangent planes is required. But these two properties differs. As described in Proposition 3.8, the spline functions that we consider have vanishing derivatives at the extraordinary vertices of the mesh (for which $N \neq 0 \pmod{4}$) and thus they are singular at these points.*

Remark 3.16. *In [19], the construction of G^1 surfaces with arbitrary topology is considered, using bicubic patches at regular vertices and bi-quintic patches at extraordinary points, in order to satisfy the G^1 constraints around these vertices. In this paper, we consider only bi-cubic patches and allow singularities at extraordinary points. A basis of the spline functions over a parametric mesh is constructed and they are used as shape functions, trial functions and test functions in the isoparametric finite element method or isogeometric analysis method. To validate the properties of these spline functions for solving the Grad-Shafranov equation, H^1 integrability assumption of parameterizations will be discussed in the next section.*

4. Parameterizations and C^1 -test functions on physical domains

In this section, we analyze the practicability of the splines defined in this paper. Based on the steps of solving the target application in the Introduction, two aspects should be considered. The first is generating a parameterization represented by the Hermite bases constructed in Section 3.2. A sketch of the algorithm is given in Section 4.1. Using this construction, we analyze the property of parameterization for solving the Grad-Shafranov equation. The second is the convergence behavior of solving PDEs. In the following examples, we take Hermite bases as shape functions, test functions and trial functions. This will be discussed in Section 5.1.

4.1. Parameterization

There are three steps for generating a parameterization \mathcal{P} that aligns curves called iso-curves.

- Based on the iso-curves, design a parametric mesh \mathcal{M} such that these iso-curves can be treated as the image of some mesh grid lines of \mathcal{M} under a parameterization;
- Choose positions $\mathbf{Q} = \{Q_i\}$ on the physical domain and their parameters $\mathbf{P} = \{P_i\}$ with frame \mathcal{F} , where we expect $\mathcal{P}(P_i) = Q_i$;
- Minimize the energy E :

$$E = \sum_{P_i \in \mathbf{P}} \omega_i \|\mathcal{P}(P_i) - Q_i\|^2, \quad (10)$$

where $\{\omega_i\}$ are weights.

Then, a parameterization $\mathcal{P} : \mathcal{M} \rightarrow \Omega$ is obtained, where Ω is a physical domain. The choice of weights follows a rule implying that the iso-curves in the physical domain can be aligned by mesh grid lines.

The following is an example. In this example, the topology of the parametric mesh is the same as that of the mesh of the target application.

Example 4.1.

The physical domain Ω shown in the left of Figure 9 is bounded by $y^2 - x(x - 1)^2 = 2$, $(x - 2)^2 + y^2 = 0.25$, $x = 2$, $(x - 0.5)^2 + y^2 = (\sqrt{2}/10)^2$. The iso-curves are given by $F0 : y^2 - x(x - 1)^2 = 0$, $F2 : y^2 - x(x - 1)^2 = 2$, $X2 : x = 2$, $C0 : (x - 0.5)^2 + y^2 = (\sqrt{2}/10)^2$ and $C1 : (x - 2)^2 + y^2 = 0.25$. Then we construct a parametric mesh \mathcal{M} shown in the left of Figure 8. Some grid lines of \mathcal{M} are expected to align the iso-curves shown on the right of Figure 8.

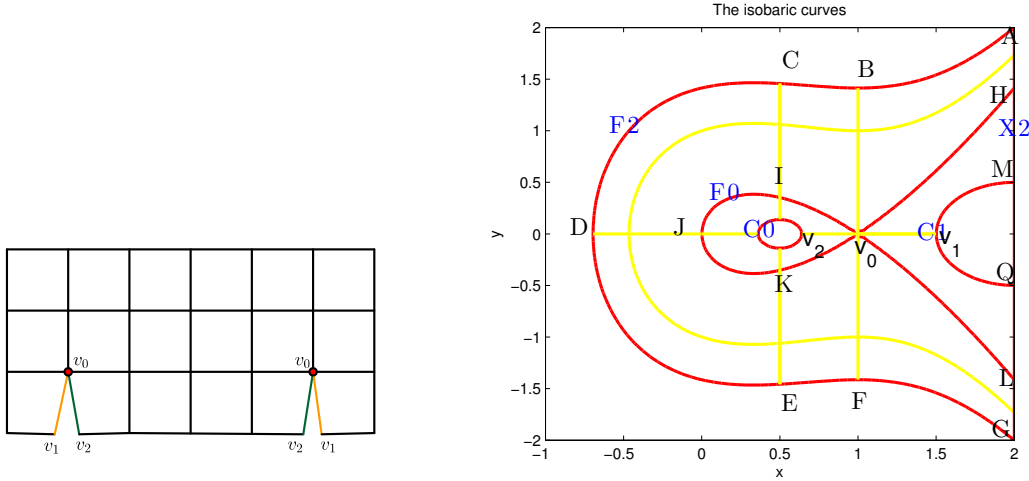


Figure 8: Parametric mesh of Example 4.1, where $\deg v_0 = 8$

Take $\mathbf{Q} = \{Q_i\}$ in Ω and $\mathbf{P} = \{P_i\}$ on \mathcal{M} , where \mathbf{Q} is shown in the middle of Figure 9. Then, minimize the energy (10) with weights of 1.5 for the points on the iso-curves and weights of 1.0 for the other points. The obtained parameterization \mathcal{P} is obtained shown on the right of Figure 9.

- Based on Example 4.1, Hermite bases can be used to represent the physical domain with complex iso-curves. However, even if there are 4 degree of freedoms at v_0 in Figure 8, there is only one degree of freedom used by the result of this algorithm. Thus, there is a singularity at v_0 , i.e., the Jacobian of this parameterization at v_0 is zero.
- To avoid a foldover, the singularities of parameterization are required at all of the interior non-hanging vertices that do not possess valence 4 (interior extraordinary vertices). In order to test a general convergence behavior of solving PDEs, in the following examples, parameterizations with singularities are chosen.

- \mathcal{P} is a parameterization, which is a bijective map. B is a basis function defined on \mathcal{M} . The corresponding test function is $B \circ \mathcal{P}^{-1}$. Then,

$$\frac{\partial(B \circ \mathcal{P}^{-1})}{\partial x} = \frac{\partial B}{\partial s} \frac{\partial s}{\partial x} + \frac{\partial B}{\partial t} \frac{\partial t}{\partial x} = \left(\frac{\partial B}{\partial s} \frac{\partial y}{\partial t} - \frac{\partial B}{\partial t} \frac{\partial y}{\partial s} \right) / \mathcal{J} \quad (11)$$

$$\frac{\partial(B \circ \mathcal{P}^{-1})}{\partial y} = \frac{\partial B}{\partial s} \frac{\partial s}{\partial y} + \frac{\partial B}{\partial t} \frac{\partial t}{\partial y} = \left(\frac{\partial x}{\partial s} \frac{\partial B}{\partial t} - \frac{\partial x}{\partial t} \frac{\partial B}{\partial s} \right) / \mathcal{J} \quad (12)$$

where $\mathcal{J} = \frac{\partial x}{\partial s} \frac{\partial y}{\partial t} - \frac{\partial x}{\partial t} \frac{\partial y}{\partial s}$. Thus, the continuity of test functions on a physical domain is determined by the parameter continuity of splines and the physical domain's parameterization. For example, if $\mathcal{J}|_U \neq 0$, then $B \circ \mathcal{P}^{-1} \in C^1(U)$, where $U \subset \mathcal{M}$. Singularities of a parameterization is a crucial issue for discussing the continuity of test functions on a physical domain. However, sometimes they cannot be avoided. For example, it is caused by the geometry of a physical domain, such as using NURBS represents a circular domain without splitting [27, 20, 21]. Moreover, in this paper, they can be caused by a loss of degree of freedoms of splines at extraordinary vertices. In this paper, we consider that the singularities of \mathcal{P} only appear at extraordinary points of \mathcal{M} and they are isolated thanks to a subdivision of an initial mesh. In Section 4.2, we will analyze the continuity of test functions where an associative parameterization is modified by the algorithm in [28].

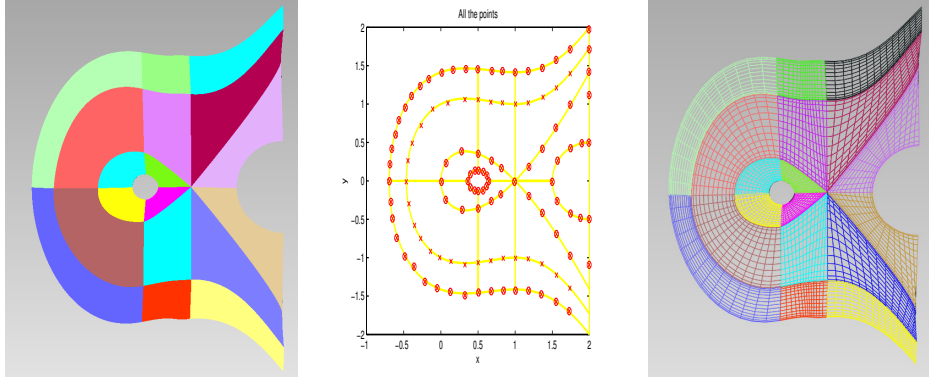


Figure 9: Physical domain (left), $\mathbf{Q} = \{Q_i\}$ (middle) and parameterization of the physical domain(right)

4.2. C^1 -test functions on physical domains

A parameterization of a physical domain used in this section is modified by the algorithm developed in [28]. It is an H^1 -parameterization, i.e., by this parameterization, the test functions are H^1 on the physical domain at least. By analysing in this

section, if C^1 -test functions are required for solving high order PDEs, we give a constraint condition at each extraordinary vertex such that all the test functions are C^1 or almost C^1 (defined in the following context). Moreover, this C^1 -constraint condition preserves the approximation property in Theorem 5.1 of Section 5.1, i.e., the optimal approximation order is reached even if there is an additional constraint condition at extraordinary vertices.

In this section, we classify all the test functions into three classes: $C^1(\Omega)$ -test functions, almost $C^1(\Omega)$ -test functions and essential $H^1(\Omega)$ -test functions. By Lemmas 4.1 and 4.2, we discuss the almost $C^1(\Omega)$ -test functions and essential $H^1(\Omega)$ -test functions respectively. In Theorem 4.3, the number and the area of supports of essential $H^1(\Omega)$ -test functions on Ω are estimated. At the end of this section, the C^1 -constraint condition is presented in Remark 4.4.

Let \mathcal{M}_0 be an initial parametric mesh. When we subdivide its cells into 4 sub-cells, the extraordinary vertices will be surrounded by the vertices whose valences are 4, and the number of extraordinary vertices will not change. For example, the topology of the initial parametric mesh is shown on the left side of Figure 10. By subdividing, the topology of the parametric mesh is shown on the right side of Figure 10. The number of extraordinary vertices does not change, and the number of cells with an extraordinary vertex as a corner vertex does not change. Let v be an extraordinary

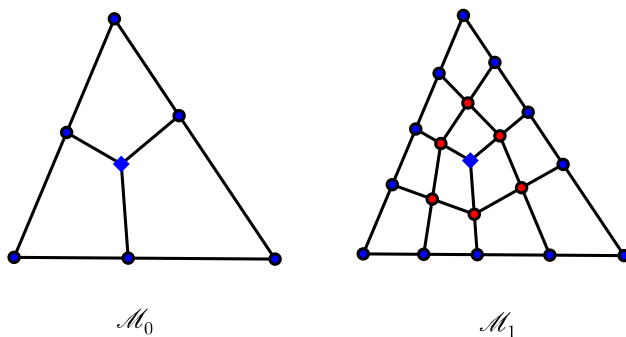


Figure 10: Subdivide the initial parametric mesh \mathcal{M}_0

vertex of the initial parametric mesh \mathcal{M}_0 . After subdividing k times uniformly, we obtain the parametric mesh \mathcal{M}_k . There are two classes of cells of \mathcal{M}_k . The first is a cell with 4 regular vertices, i.e., all of the vertices are boundary vertices, or their valences are 4, the second is a cell with one extraordinary vertex as its vertex. The test functions are divided into the following three classes.

- $C^1(\Omega)$: a test function $B \circ \mathcal{P}^{-1}$ is called a $C^1(\Omega)$ -test function, if $B \circ \mathcal{P}^{-1}$,

$\frac{\partial(B \circ \mathcal{P}^{-1})}{\partial x}$ and $\frac{\partial(B \circ \mathcal{P}^{-1})}{\partial y}$ are continuous on Ω

- Almost $C^1(\Omega)$: a test function $B \circ \mathcal{P}^{-1}$ is called an almost $C^1(\Omega)$ -test function, if $B \circ \mathcal{P}^{-1}$ is continuous on Ω . Besides the isolated singularities of \mathcal{P} , $\frac{\partial(B \circ \mathcal{P}^{-1})}{\partial x}$ and $\frac{\partial(B \circ \mathcal{P}^{-1})}{\partial y}$ are continuous on Ω and for each singularity p_0 ,

$$\lim_{p \rightarrow p_0} \frac{\partial(B \circ \mathcal{P}^{-1})}{\partial x} \text{ and } \lim_{p \rightarrow p_0} \frac{\partial(B \circ \mathcal{P}^{-1})}{\partial y}$$

exist, where $p \in \Omega$ is an image of an interior point of a cell of \mathcal{M}_k by \mathcal{P} .

- Essential $H^1(\Omega)$: a test function $B \circ \mathcal{P}^{-1}$ is called an essential $H^1(\Omega)$ -test function, if $B \circ \mathcal{P}^{-1}$ is continuous on Ω . Besides the isolated singularities of \mathcal{P} , $\frac{\partial(B \circ \mathcal{P}^{-1})}{\partial x}$ and $\frac{\partial(B \circ \mathcal{P}^{-1})}{\partial y}$ are continuous on Ω , $B \circ \mathcal{P}^{-1} \in H^1(\Omega)$ and for each singularity p_0 ,

$$\lim_{p \rightarrow p_0} \frac{\partial(B \circ \mathcal{P}^{-1})}{\partial x} \text{ or } \lim_{p \rightarrow p_0} \frac{\partial(B \circ \mathcal{P}^{-1})}{\partial y}$$

doesn't exist where $p \in \Omega$ is an image of an interior point of a cell of \mathcal{M}_k by \mathcal{P}

Lemma 4.1. *Let v_0 be an extraordinary vertex of \mathcal{M}_k and $p_0 = \mathcal{P}(v_0)$. If B satisfies*

$$\frac{\partial B}{\partial s}(v_0) = 0, \quad \frac{\partial B}{\partial t}(v_0) = 0 \text{ and } \frac{\partial^2 B}{\partial s \partial t}(v_0) = 0,$$

then $B \circ \mathcal{P}^{-1}$ is an almost $C^1(\Omega)$ -test function, where \mathcal{P} is an H^1 -parameterization.

Proof. Let C be a cell of \mathcal{M}_k and v_0 be C 's vertex. Suppose that (\mathbf{s}, \mathbf{t}) is the local frame of C and $\mathcal{P}|_C = (x(s, t), y(s, t))$. Then, based on Theorem 3.2 in [28],

$$\frac{\partial x}{\partial s}(v_0) = 0, \quad \frac{\partial x}{\partial t}(v_0) = 0, \quad \frac{\partial^2 x}{\partial s \partial t}(v_0) = 0, \quad \frac{\partial y}{\partial s}(v_0) = 0, \quad \frac{\partial y}{\partial t}(v_0) = 0, \quad \frac{\partial^2 y}{\partial s \partial t}(v_0) = 0,$$

For $v \in C^\circ$, $\mathbf{l} = \overrightarrow{v_0 v}$, where C° is the interior of C . Then, if a function $f(s, t)$ satisfies $\frac{\partial f}{\partial s}(v_0) = 0$, $\frac{\partial^2 f}{\partial s \partial t}(v_0) = 0$, then, by Taylor expansion along \mathbf{l} , there is a point v_f on the segment $v_0 v$ such that

$$\frac{\partial f}{\partial s}(v) = \frac{\partial f}{\partial s}(v_0) + \frac{\partial^2 f}{\partial s \partial \mathbf{l}}(v_f) \ell = \frac{\partial^2 f}{\partial s^2}(v_f) \ell \cos \theta + \frac{\partial^2 f}{\partial s \partial t}(v_f) \ell \sin \theta, \quad (13)$$

where θ is the angle between \mathbf{s} and \mathbf{l} , $\ell = |v_0 v|$. By $\partial^2 f(v_0)/\partial s \partial t = 0$ and Taylor expansion, there is a point v_f^0 on the segment $v_0 v_f$ (a part of $v_0 v$) such that

$$\frac{\partial^2 f}{\partial s \partial t}(v_f) = \frac{\partial^2 f}{\partial s \partial t}(v_0) + \frac{\partial^3 f}{\partial s \partial t \partial \mathbf{l}}(v_f^0) \ell_1 = o(1),$$

where $\ell_1 = |v_0 v_f| < \ell$. By (13),

$$\frac{\partial f}{\partial s}(v) = \frac{\partial^2 f}{\partial s^2}(v_f) \ell \cos \theta + o(\ell). \quad (14)$$

By the same method, if $f(s, t)$ satisfies $\frac{\partial f}{\partial t}(v_0) = 0$, $\frac{\partial^2 f}{\partial s \partial t}(v_0) = 0$, then

$$\frac{\partial f}{\partial t}(v) = \frac{\partial^2 f}{\partial t^2}(v_f) \ell \sin \theta + o(\ell). \quad (15)$$

While B , $x(s, t)$ and $y(s, t)$ satisfy $\frac{\partial f}{\partial s}(v_0) = 0$, $\frac{\partial f}{\partial t}(v_0) = 0$, $\frac{\partial^2 f}{\partial s \partial t}(v_0) = 0$,

$$\begin{aligned} \frac{\partial(B \circ \mathcal{P}^{-1})}{\partial x} &= \frac{\partial B}{\partial s} \frac{\partial s}{\partial x} + \frac{\partial B}{\partial t} \frac{\partial t}{\partial x} = \left(\frac{\partial B}{\partial s} \frac{\partial y}{\partial t} - \frac{\partial B}{\partial t} \frac{\partial y}{\partial s} \right) / \left(\frac{\partial x}{\partial s} \frac{\partial y}{\partial t} - \frac{\partial x}{\partial t} \frac{\partial y}{\partial s} \right) \\ &= \frac{\left(\frac{\partial^2 B}{\partial s^2} \Big|_{v_{Bs}} \frac{\partial^2 y}{\partial t^2} \Big|_{v_{yt}} - \frac{\partial^2 B}{\partial t^2} \Big|_{v_{Bt}} \frac{\partial^2 y}{\partial s^2} \Big|_{v_{ys}} \right) \sin \theta \cos \theta \ell^2 + o(\ell^2)}{\left(\frac{\partial^2 x}{\partial s^2} \Big|_{v_{xs}} \frac{\partial^2 y}{\partial t^2} \Big|_{v_{yt}^0} - \frac{\partial^2 x}{\partial t^2} \Big|_{v_{xt}} \frac{\partial^2 y}{\partial s^2} \Big|_{v_{ys}^0} \right) \sin \theta \cos \theta \ell^2 + o(\ell^2)} \\ &= \frac{\left(\frac{\partial^2 B}{\partial s^2} \Big|_{v_{Bs}} \frac{\partial^2 y}{\partial t^2} \Big|_{v_{yt}} - \frac{\partial^2 B}{\partial t^2} \Big|_{v_{Bt}} \frac{\partial^2 y}{\partial s^2} \Big|_{v_{ys}} \right) + o(\ell^2) / (\sin \theta \cos \theta \ell^2)}{\left(\frac{\partial^2 x}{\partial s^2} \Big|_{v_{xs}} \frac{\partial^2 y}{\partial t^2} \Big|_{v_{yt}^0} - \frac{\partial^2 x}{\partial t^2} \Big|_{v_{xt}} \frac{\partial^2 y}{\partial s^2} \Big|_{v_{ys}^0} \right) + o(\ell^2) / (\sin \theta \cos \theta \ell^2)} \\ &= \frac{\left(\frac{\partial^2 B}{\partial s^2} \Big|_{v_{Bs}} \frac{\partial^2 y}{\partial t^2} \Big|_{v_{yt}} - \frac{\partial^2 B}{\partial t^2} \Big|_{v_{Bt}} \frac{\partial^2 y}{\partial s^2} \Big|_{v_{ys}} \right) + o(1)}{\left(\frac{\partial^2 x}{\partial s^2} \Big|_{v_{xs}} \frac{\partial^2 y}{\partial t^2} \Big|_{v_{yt}^0} - \frac{\partial^2 x}{\partial t^2} \Big|_{v_{xt}} \frac{\partial^2 y}{\partial s^2} \Big|_{v_{ys}^0} \right) + o(1)}, \end{aligned}$$

where $\sin \theta \cos \theta \neq 0$ because $v \in C^o$. Thus,

$$\lim_{p \rightarrow p_0} \frac{\partial(B \circ \mathcal{P}^{-1})}{\partial x} = \lim_{v \rightarrow v_0} \frac{\left(\frac{\partial^2 B}{\partial s^2} \Big|_{v_{Bs}} \frac{\partial^2 y}{\partial t^2} \Big|_{v_{yt}} - \frac{\partial^2 B}{\partial t^2} \Big|_{v_{Bt}} \frac{\partial^2 y}{\partial s^2} \Big|_{v_{ys}} \right) + o(1)}{\left(\frac{\partial^2 x}{\partial s^2} \Big|_{v_{xs}} \frac{\partial^2 y}{\partial t^2} \Big|_{v_{yt}^0} - \frac{\partial^2 x}{\partial t^2} \Big|_{v_{xt}} \frac{\partial^2 y}{\partial s^2} \Big|_{v_{ys}^0} \right) + o(1)}, \quad (16)$$

where $p_0 = \mathcal{P}(v_0)$. Moreover,

$$\lim_{v \rightarrow v_0} \left(\frac{\partial^2 B}{\partial s^2} \Big|_{v_{Bs}} \frac{\partial^2 y}{\partial t^2} \Big|_{v_{yt}} - \frac{\partial^2 B}{\partial t^2} \Big|_{v_{Bt}} \frac{\partial^2 y}{\partial s^2} \Big|_{v_{ys}} \right) + o(1) = \frac{\partial^2 B}{\partial s^2} \Big|_{v_0} \frac{\partial^2 y}{\partial t^2} \Big|_{v_0} - \frac{\partial^2 B}{\partial t^2} \Big|_{v_0} \frac{\partial^2 y}{\partial s^2} \Big|_{v_0},$$

and,

$$\lim_{v \rightarrow v_0} \left(\frac{\partial^2 x}{\partial s^2} \Big|_{v_{x_s}} \frac{\partial^2 y}{\partial t^2} \Big|_{v_{y_t}^0} - \frac{\partial^2 x}{\partial t^2} \Big|_{v_{x_t}} \frac{\partial^2 y}{\partial s^2} \Big|_{v_{y_s}^0} \right) + o(1) = \frac{\partial^2 x}{\partial s^2} \Big|_{v_0} \frac{\partial^2 y}{\partial t^2} \Big|_{v_0} - \frac{\partial^2 x}{\partial t^2} \Big|_{v_0} \frac{\partial^2 y}{\partial s^2} \Big|_{v_0}.$$

$\frac{\partial^2 x}{\partial s^2} \Big|_{v_0} \frac{\partial^2 y}{\partial t^2} \Big|_{v_0} - \frac{\partial^2 x}{\partial t^2} \Big|_{v_0} \frac{\partial^2 y}{\partial s^2} \Big|_{v_0} \neq 0$ because $\frac{\partial^2 x}{\partial s^2} \Big|_{v_0} \frac{\partial^2 y}{\partial t^2} \Big|_{v_0} - \frac{\partial^2 x}{\partial t^2} \Big|_{v_0} \frac{\partial^2 y}{\partial s^2} \Big|_{v_0} = 16 \|\overrightarrow{\mathbf{P}_2 \mathbf{P}_1} \times \overrightarrow{\mathbf{P}_4 \mathbf{P}_1}\|$ and $\overrightarrow{\mathbf{P}_2 \mathbf{P}_1}, \overrightarrow{\mathbf{P}_4 \mathbf{P}_1}$ are non-collinear in Theorem 3.2 of [28]. Thus,

$$\lim_{p \rightarrow p_0} \frac{\partial(B \circ \mathcal{P}^{-1})}{\partial x} = \frac{\frac{\partial^2 B}{\partial s^2} \Big|_{v_0} \frac{\partial^2 y}{\partial t^2} \Big|_{v_0} - \frac{\partial^2 B}{\partial t^2} \Big|_{v_0} \frac{\partial^2 y}{\partial s^2} \Big|_{v_0}}{\frac{\partial^2 x}{\partial s^2} \Big|_{v_0} \frac{\partial^2 y}{\partial t^2} \Big|_{v_0} - \frac{\partial^2 x}{\partial t^2} \Big|_{v_0} \frac{\partial^2 y}{\partial s^2} \Big|_{v_0}}.$$

By the same method,

$$\lim_{p \rightarrow p_0} \frac{\partial(B \circ \mathcal{P}^{-1})}{\partial y} = \frac{\frac{\partial^2 x}{\partial s^2} \Big|_{v_0} \frac{\partial^2 B}{\partial t^2} \Big|_{v_0} - \frac{\partial^2 x}{\partial t^2} \Big|_{v_0} \frac{\partial^2 B}{\partial s^2} \Big|_{v_0}}{\frac{\partial^2 x}{\partial s^2} \Big|_{v_0} \frac{\partial^2 y}{\partial t^2} \Big|_{v_0} - \frac{\partial^2 x}{\partial t^2} \Big|_{v_0} \frac{\partial^2 y}{\partial s^2} \Big|_{v_0}}.$$

So, $B \circ \mathcal{P}^{-1}$ is an almost $C^1(\Omega)$ -test function. \square

Lemma 4.2. *Let v_0 be an extraordinary vertex of \mathcal{M}_k and $p_0 = \mathcal{P}(v_0)$. If B satisfies*

$$\frac{\partial B}{\partial s}(v_0) \neq 0 \text{ or } \frac{\partial B}{\partial t}(v_0) \neq 0$$

then $B \circ \mathcal{P}^{-1}$ is an essential H^1 -test function, where \mathcal{P} is an H^1 -parameterization.

Proof. By the same analysis as Lemma 4.1, if $\frac{\partial B}{\partial s}(v_0) \neq 0$,

$$\begin{aligned} \frac{\partial(B \circ \mathcal{P}^{-1})}{\partial x} &= \frac{\partial B}{\partial s} \frac{\partial s}{\partial x} + \frac{\partial B}{\partial t} \frac{\partial t}{\partial x} = \left(\frac{\partial B}{\partial s} \frac{\partial y}{\partial t} - \frac{\partial B}{\partial t} \frac{\partial y}{\partial s} \right) / \left(\frac{\partial x}{\partial s} \frac{\partial y}{\partial t} - \frac{\partial x}{\partial t} \frac{\partial y}{\partial s} \right) \\ &= \frac{\frac{\partial B}{\partial s} \Big|_v \frac{\partial^2 y}{\partial s^2} \Big|_{v_{y_s}} \sin \theta \ell + o(\ell)}{\left(\frac{\partial^2 x}{\partial s^2} \Big|_{v_{x_s}} \frac{\partial^2 y}{\partial t^2} \Big|_{v_{y_t}^0} - \frac{\partial^2 x}{\partial t^2} \Big|_{v_{x_t}} \frac{\partial^2 y}{\partial s^2} \Big|_{v_{y_s}^0} \right) \sin \theta \cos \theta \ell^2 + o(\ell^2)} \\ &= \frac{\frac{\partial B}{\partial s} \Big|_v \frac{\partial^2 y}{\partial s^2} \Big|_{v_{y_s}} \sin \theta + o(1)}{\left(\frac{\partial^2 x}{\partial s^2} \Big|_{v_{x_s}} \frac{\partial^2 y}{\partial t^2} \Big|_{v_{y_t}^0} - \frac{\partial^2 x}{\partial t^2} \Big|_{v_{x_t}} \frac{\partial^2 y}{\partial s^2} \Big|_{v_{y_s}^0} \right) \sin \theta \cos \theta \ell + o(\ell)} \end{aligned}$$

When $p \rightarrow p_0$, $\ell \rightarrow 0$. Thus $\lim_{p \rightarrow p_0} \frac{\partial(B \circ \mathcal{P}^{-1})}{\partial x}$ doesn't exist. If B satisfies $\frac{\partial B}{\partial t}(v_0) \neq 0$, the same result can be obtained.

While \mathcal{P} satisfies H^1 integrability assumption. i.e., $B \circ \mathcal{P} \in H^1(\Omega)$. Thus $B \circ \mathcal{P}^{-1}$ is an essential H^1 -test function. \square

Theorem 4.3. *Let \mathcal{M}_0 be an initial parametric mesh. There are n_{ir} extraordinary vertices and m cells. \mathcal{M}_k is the mesh obtained by subdividing \mathcal{M}_0 k times uniformly. Then, $n_{H^1}/n \sim O(\frac{1}{k^2})$ and $A_{H^1}(\Omega) \sim O(h^4)$, where n_{H^1} is the number of essential $H^1(\Omega)$ -test functions, n is the number of all test functions, $A_{H^1}(\Omega)$ is the sum of the area of all of essential $H^1(\Omega)$ -test functions' supports, $h = 1/(k + 1)$ and \mathcal{P} is an H^1 -parameterization.*

Proof. Let B be a Hermite basis defined on \mathcal{M}_k in Section 3.2 and its support is denoted as $\text{supp}(B)$. If there is no extraordinary vertex in $\overline{\text{supp}(B)}$, then $B \circ \mathcal{P}^{-1}$ is $C^1(\Omega)$. Thus, in the following, the continuity of $B \circ \mathcal{P}^{-1}$ is discussed, where there is an extraordinary vertex in $\overline{\text{supp}(B)}$. Two kinds of Hermite bases should be considered. Let v_0 be an extraordinary vertex.

1. B is associated to a vertex that has a common cell with v_0 . For this case,

$$\frac{\partial B}{\partial s}(v_0) = 0, \quad \frac{\partial B}{\partial t}(v_0) = 0, \quad \text{and} \quad \frac{\partial^2 B}{\partial s \partial t}(v_0) = 0,$$

by Lemma 4.1, $B \circ \mathcal{P}^{-1}$ is an almost $C^1(\Omega)$ -test function.

2. B is associated to v_0 . If B 's Hermite data corresponds to $[1, 0, 0, 0]$, by Lemma 4.1, $B \circ \mathcal{P}^{-1}$ is an almost $C^1(\Omega)$ -test function. By Lemma 4.2, if B 's Hermite data corresponds to $[0, 1, 0, 0]$ or $[0, 0, 1, 0]$, then $B \circ \mathcal{P}^{-1}$ is an essential H^1 -test function. If B 's Hermite data corresponds to $[0, 0, 0, 1]$, by the same analysis as Lemmas 4.1 and 4.2, the continuity of $B \circ \mathcal{P}^{-1}(\in H^1(\Omega))$ depends on the positions of the 1-neighbourhood vertices of v_0 .

The number of these essential $H^1(\Omega)$ -test functions doesn't change when we subdivide the initial mesh \mathcal{M}_0 . The number of essential $H^1(\Omega)$ -test functions is less than $3n_{ir}$. By subdividing each cell of \mathcal{M}_0 into k^2 uniform subcells, there are at least $(k - 1)^2$ regular vertices, i.e, the number of test functions at least $4(k - 1)^2$. Thus, $n_{H^1}/n \sim O(\frac{1}{k^2})$.

The number of cells that take an extraordinary vertex as their corners doesn't change when $k > 1$. Thus, for $A_{H^1}(\Omega)$, we just compute the area of the image of one of these cells on a physical domain by \mathcal{P} . For one cell, its size is $h \times h$ on the parametric domain and the Jacobian of \mathcal{P} is $O(h^2)$, where $h = 1/(k + 1)$. Thus, the area of its image on the physical domain is $O(h^4)$, i.e, $A_{H^1}(\Omega) \sim O(h^4)$. \square

Remark 4.4. 1. *Most of test functions are C^1 or almost C^1 , i.e., $n_{C^1}/n \sim O(1)$, where n_{C^1} is the number of C^1 -test functions and almost C^1 -test functions.*

2. $A_{H^1}(\Omega) \sim O(h^4)$. $A_{H^1}(\Omega)$ has the same order as the approximation order in Theorem 5.1 by Hermite bases.

3. *For a global C^1 numerical solution on a physical domain, a constraint condition is added at extraordinary vertices such that the coefficients of splines corresponding to essential $H^1(\Omega)$ -test functions are set as zeros. This constraint is called **C^1 -constraint condition** and it keeps the result in Theorem 5.1. Because we just use the Hermite*

bases according to $[1, 0, 0, 0]$ at extraordinary vertices to construct the approximation function of $F(x, y) \in C^4(\Omega)$ in the proof of Theorem 5.1.

5. Convergence behavior with bicubic Hermite bases

Usually, based on the classical FEM error analysis (Theorem 6.2.1 and Proposition 6.2.2 in [22]), if the exact solution $u \in H^4(\Omega)$, error orders with L^2 -norm as 4 and with H^1 -norm as 3 are expected when we use bicubic splines as trial functions. In this section, the Hermite bases constructed in Section 3.2 are used to represent the parameterizations of physical domains, and they are treated as trial and test functions when solving the model PDE. To analyze the convergence behavior of Hermite bases, an interpolation approximation error measured by L^2 -norm is discussed in Section 5.1. The optimal approximation rate is reached. In Section 5.2, several numerical examples for solving the Grad-shafanov equation are presented to verify the numerical convergence rates measured by L^2 -norm and H^1 -norm.

5.1. The interpolation approximation error by bicubic Hermite bases

In this section, the interpolation approximation error by bicubic Hermite bases is presented.

Theorem 5.1. *Let $\mathcal{P} : \mathcal{M}_k \rightarrow \Omega$ be a parameterization (an injective map) represented by Hermite bases over \mathcal{M}_k and $\Omega = \mathcal{P}(\mathcal{M}_k)$. Suppose that $F(x, y) \in C^4(\Omega)$. Then there is a $u \in \mathbf{S}(3, 1; \mathcal{M}_k)$ such that*

$$\|U(x, y) - F(x, y)\|_{L^2} \leq Kh^4,$$

where $K \in \mathbb{R}_+$, $U(x, y) = u \circ \mathcal{P}^{-1}$, \mathcal{M}_0 is an initial parametric mesh and the size of each cell of \mathcal{M}_0 is 1×1 , \mathcal{M}_k is the parametric mesh obtained by subdividing \mathcal{M}_0 k times uniformly, $h = 1/(k + 1)$.

Proof. First, we construct $u \in \mathbf{S}(3, 1; \mathcal{M}_k)$. For each vertex v_i of \mathcal{M}_k , $F \circ \mathcal{P}$'s Hermite data can be used to recover a spline defined over \mathcal{M}_k . To be specific, let $C = [s_1, s_1 + h] \times [t_1, t_1 + h]$ be a cell with v_i as its vertex, where $h = 1/(k + 1)$.

- If v_i 's valence is 4 or v_i is a boundary vertex, i.e. v_i is regular, the coefficients of the 4 Hermite bases can be obtained by

$$\left[F \circ \mathcal{P}|_C(v_i), \frac{\partial F \circ \mathcal{P}|_C}{\partial s}(v_i), \frac{\partial F \circ \mathcal{P}|_C}{\partial t}(v_i), \frac{\partial^2 F \circ \mathcal{P}|_C}{\partial s \partial t}(v_i) \right],$$

where (s, t) is the coordinates associated with C ;

- Otherwise, the coefficients of 4 Hermite bases can be obtained by

$$[F \circ \mathcal{P}(v_i), 0, 0, 0].$$

Thus, we define a spline function u over \mathcal{M}_k as the linear combination of the Hermite basis with coefficients corresponding to these values.

Let $U = u \circ \mathcal{P}^{-1}$. We estimate the L^2 error

$$\begin{aligned} \|U(x, y) - F(x, y)\|_{L^2}^2 &= \int_{\Omega} (U(x, y) - F(x, y))^2 dx dy \\ &= \sum_{C_i^1} \int_{\mathcal{P}(C_i^1)} (U(x, y) - F(x, y))^2 dx dy + \sum_{C_i^2} \int_{\mathcal{P}(C_i^2)} (U(x, y) - F(x, y))^2 dx dy \end{aligned} \quad (17)$$

where C_i^1 is a cell with 4 regular vertices and C_i^2 is a cell with one extraordinary vertex as its vertex. We will estimate $\int_{\mathcal{P}(C_i^1)} (U(x, y) - F(x, y))^2 dx dy$ and $\int_{\mathcal{P}(C_i^2)} (U(x, y) - F(x, y))^2 dx dy$, respectively.

Case 1: There are 4 Hermite bases at each regular vertex of cell $C_i^1 = [s_1, s_1 + h] \times [t_1, t_1 + h]$ of \mathcal{M}_k . Then $u|_{C_i^1}$'s Hermite data at each vertex of C_i^1 is the same as the Hermite data of $F \circ \mathcal{P}|_{C_i^1}$ at these vertices. Because $F(x, y) \in C^4(\Omega)$ and each component of $\mathcal{P}|_{C_i^1}$ is a bicubic polynomial. $F \circ \mathcal{P}|_{C_i^1} \in C^4(C_i^1)$. By Theorem 4 in [23],

$$|F \circ \mathcal{P}|_{C_i^1}(s, t) - u(s, t)| \leq K_1 h^4, \quad (18)$$

where K_1 is a const, $u(s, t) = u|_{C_i^1}(s, t)$. Thus,

$$\int_{\mathcal{P}(C_i^1)} (F(x, y) - U(x, y))^2 dx dy = \int_{C_i^1} (F \circ \mathcal{P}|_{C_i^1}(s, t) - u|_{C_i^1}(s, t))^2 |\mathcal{J}_{C_i^1}(s, t)| ds dt$$

where

$$\mathcal{J}_{C_i^1}(s, t) = \begin{vmatrix} \frac{\partial x(s, t)}{\partial t} & \frac{\partial x(s, t)}{\partial s} \\ \frac{\partial y(s, t)}{\partial t} & \frac{\partial y(s, t)}{\partial s} \end{vmatrix}$$

with $\mathcal{P}|_{C_i^1}(s, t) = [x(s, t), y(s, t)]$. There is a constant K_2 such that

$$|\mathcal{J}_{C_i^1}(s, t)| \leq K_2.$$

Thus

$$\begin{aligned} \int_{\mathcal{P}(C_i^1)} (F(x, y) - U(x, y))^2 dx dy &\leq K_1 K_2 (h^4)^2 \int_{C_i^1} ds dt \\ &= K_1 K_2 h^{10}, \end{aligned}$$

Owing to the subdivision, the number of this type of cell of \mathcal{M}_{k+1} is less than $N_r(k+1)^2 = N_r/h^2$. Thus,

$$\begin{aligned} \sum_{C_i^1} \int_{\mathcal{P}(C_i^1)} (U(x, y) - F(x, y))^2 dx dy &\leq K_1 K_2 h^{10} * (N_r/h^2) \\ &= K_1 K_2 N_r h^8, \end{aligned} \quad (19)$$

where N_r is the number of cells of \mathcal{M}_0 .

Case 2: Let C_i^2 be a cell that takes an extraordinary vertex v as one of its vertices. Then the other three vertices v_1, v_2, v_3 of C_i^2 are the vertices with valence 4. Suppose $C_i^2 = [s_1, s_1 + h] \times [t_1, t_1 + h]$, $v_1(s_1, t_1), v_2(s_1 + h, t_1), v_3(s_1, t_1 + h), v(s_1 + h, t_1 + h)$. Then the spline u defined over \mathcal{M}_k satisfies

- $u(v) = F \circ \mathcal{P}(v)$;
- $H_{(s,t)}^{v_i}(u) = H_{(s,t)}^{v_i}(F \circ \mathcal{P})$, i. e. ,

$$\begin{aligned} u(v_i) &= F \circ \mathcal{P}(v_i); & \frac{\partial u(v_i)}{\partial s} &= \frac{\partial F \circ \mathcal{P}(v_i)}{\partial s}; \\ \frac{\partial u(v_i)}{\partial t} &= \frac{\partial F \circ \mathcal{P}(v_i)}{\partial t}; & \frac{\partial^2 u(v_i)}{\partial s \partial t} &= \frac{\partial^2 F \circ \mathcal{P}(v_i)}{\partial s \partial t}, \end{aligned}$$

where $i = 1, 2, 3$.

Denote $\psi(s, t) = F \circ \mathcal{P}|_{C_i^2}(s, t) - u|_{C_i^2}(s, t)$, then,

$$\psi(v_1) = 0, \frac{\partial \psi}{\partial s}(v_1) = 0, \frac{\partial \psi}{\partial t}(v_1) = 0.$$

By Taylor expansion at v_1 , there is $v_p \in C_i^2$ such that

$$\psi(s, t) = \frac{1}{2!} \frac{\partial^2 \psi}{\partial \mathbf{l}^2}(v_p)(s - s_0)(t - t_0),$$

where $\mathbf{l} = v_p \vec{v}_1 / |v_p \vec{v}_1|$. There is a const C such that

$$\left| \frac{\partial^2 \psi}{\partial \mathbf{l}^2}(v_p) \right| \leq C$$

when $\psi(s, t) \in C^4$. Thus, there is a positive constant K_3 such that

$$|F \circ \mathcal{P}|_{C_i^2}(s, t) - u|_{C_i^2}(s, t)| \leq K_3 h^2. \quad (20)$$

Suppose $\mathcal{P}|_{C_i^2}(s, t) = [x(s, t), y(s, t)]$. The singularity of \mathcal{P} is required at v because v is an extraordinary vertex, i.e.,

$$\begin{aligned} \frac{\partial x(v)}{\partial s} &= 0, & \frac{\partial x(v)}{\partial t} &= 0; \\ \frac{\partial y(v)}{\partial s} &= 0, & \frac{\partial y(v)}{\partial t} &= 0. \end{aligned}$$

By Taylor expansion the Jacobian of \mathcal{P} over C_i^2 is

$$\mathcal{J}_{C_i^2}(s, t) = \left| \begin{array}{cc} \frac{\partial x(s, t)}{\partial s} & \frac{\partial x(s, t)}{\partial t} \\ \frac{\partial y(s, t)}{\partial s} & \frac{\partial y(s, t)}{\partial t} \end{array} \right| \sim h^2.$$

Thus there is a positive constant K_4 such that

$$\begin{aligned} \int_{\mathcal{P}(C_i^2)} (U(x, y) - F(x, y))^2 dx dy &= \int_{C_i^2} (F \circ \mathcal{P}|_{C_i^2}(s, t) - u|_{C_i^2}(s, t))^2 |\mathcal{J}_{C_i^2}(s, t)| ds dt \\ &\leq K_4 h^6 \int_{C_i^2} ds dt \\ &= K_4 h^8. \end{aligned}$$

Due to the subdivision process, the number of the second type of cells does not change, i.e., it is a positive constant denoted as N_{ir} for each \mathcal{M}_k . Thus, there is a positive constant K_5 such that

$$\sum_{C_i^2} \int_{\mathcal{P}(C_i^2)} (U(x, y) - F(x, y))^2 dx dy \leq N_{ir} K_4 h^8 = K_5 h^8. \quad (21)$$

Based on (19) and (21), there is a positive constant K_6 such that

$$\begin{aligned} E^2 &= \int_{\Omega} (U(x, y) - F(x, y))^2 dx dy \\ &= \sum_{C_i^1} \int_{\mathcal{P}(C_i^1)} (U(x, y) - F(x, y))^2 dx dy + \sum_{C_i^2} \int_{\mathcal{P}(C_i^2)} (U(x, y) - F(x, y))^2 dx dy \quad (22) \\ &\leq K_6 h^8. \end{aligned}$$

By (22), for $F(x, y) \in C^4(\Omega)$, there is a spline u defined over \mathcal{M}_k such that

$$\|U(x, y) - F(x, y)\|_{L^2} = \sqrt{\int_{\Omega} (U(x, y) - F(x, y))^2 dx dy} \leq K h^4,$$

where $U(x, y) = u \circ \mathcal{P}^{-1}(x, y)$, K is a positive const. In other words, for a smooth function $F(x, y)$ defined over the physical domain, there is a spline u defined over \mathcal{M}_k that can be used to approximate $F(x, y)$ by an injective parameterization \mathcal{P} with an error order of 4. \square

5.2. Numerical convergence rates by bicubic Hermite bases

In this section, some examples are presented to test the convergence rate for solving PDEs caused by spline space in this paper. The reasons for choosing these examples are the following.

1. The physical domain can be exactly described by the parameterization with Hermite bases. The error between the exact solution and the solution given by the isoparametric finite element method or isogeometric analysis comes from two parts. One is the approximation error of the trail functions. The other is the approximation error of the physical domain by the shape functions. Thus, to test the error orders that come from

the approximation of our spline spaces of solving PDEs, we choose physical domains that can be exactly described by Hermite bases.

2. The Grad-Shafranov equation [24] is chosen as the model PDE problem. In [15], isoparametric bicubic Hermite elements are used to solve the Grad-Shafranov equation over a physical domain with concentric-circle-like iso-curves. They introduced a polar-coordinate-like transformation to construct a global coordinate system to achieve the desirable properties of the classical cubic Hermite element [16]. By splines defined in this paper, a general physical domain with complex iso-curves can be described globally, not only for a physical domain with concentric-circle-like iso-curves. For the continuity of the numerical solution and its gradients, the errors with L^2 -norm and H^1 -norm are presented as [1]. Let Ω be a physical domain. The generic form of the fixed-boundary Grad-Shafranov equation can be written as

$$\begin{aligned}\Delta^*u &= f_0(u, r, z) \quad \text{in } \Omega \\ u &= 0 \quad \text{on } \partial\Omega\end{aligned}\tag{23}$$

where

$$\begin{aligned}\Delta^*u &= r \frac{\partial}{\partial r} \left(\frac{1}{r} \frac{\partial u}{\partial r} \right) + \frac{\partial^2 u}{\partial z^2} \\ &= r \nabla(X \nabla u),\end{aligned}$$

and

$$X = \begin{pmatrix} 1/r & 0 \\ 0 & 1/r \end{pmatrix}$$

Thus, in the following examples, we consider

$$\begin{aligned}-\nabla(R(r)\nabla u) &= -g(r)f(u, r, z) \quad \text{in } \Omega, \\ u &= 0 \quad \text{on } \partial\Omega,\end{aligned}\tag{24}$$

where $g(r) \in L^2(\Omega)$ is a function of r and

$$R(r) = \begin{pmatrix} g(r) & 0 \\ 0 & g(r) \end{pmatrix}.$$

Case 1. If $f(u, r, z) = f(r, z) \in L^2(\Omega)$, i.e., $f(u, r, z)$ has no relationship with u , then the weak form of this model PDE (24) can be stated as follows. Given f , find $u \in V$, such that for all $v \in V$,

$$a(u, v) = l(v),\tag{25}$$

where $V = \{v : v \in \mathbf{H}^1(\Omega), v|_{\partial\Omega} = 0\}$, $\mathbf{H}^1(\Omega)$ is the Sobolev space that consists of the functions in $\mathbf{L}^2(\Omega)$ that possess weak and square-integrable derivatives. $a(u, v)$ is the symmetric bilinear form defined as

$$a(u, v) = \int_{\Omega} \nabla v^T R(r) \nabla u \, d\Omega,$$

$l(v)$ is a linear continuous functional defined as

$$l(v) = - \int_{\Omega} g(r) f(r, z) v \, d\Omega.$$

We discretize the weak form, Eq. (25), with our splines. This yields the linear system

$$\mathbf{A}\mathbf{d} = \mathbf{F}, \tag{26}$$

where \mathbf{A} is the stiffness matrix, \mathbf{F} is the force vector and \mathbf{d} is the displacement vector. **Case 2.** For a general $f(u, r, z)$ such that (24) is a nonlinear Grad-Shafranov equation, the fixed-point iteration method [26] is used to compute the solution. Take $u_0(r, z)$ as an initial solution. Suppose that the i -th iteration solution $u_i(r, z)$ has been obtained. Solve the $(i + 1)$ -th iteration solution $u_{i+1}(r, z)$ with

$$\begin{aligned} -\nabla(R(r)\nabla u_{i+1}(r, z)) &= -g(r)f(u_i(r, z), r, z) \quad \text{in } \Omega, \\ u_{i+1} &= 0 \quad \text{on } \partial\Omega, \end{aligned}$$

by the method presented in Case 1. Then the solution of model PDE (24) is given by

$$u(r, z) = \lim_{i \rightarrow \infty} u_i(r, z)$$

3. Extraordinary vertices of the initial parameter meshes of these examples are isolated. And the initial parameterizations are satisfy H^1 integrability assumption with $\alpha = (2, 2)$ and $\mathbf{p} = (3, 3)$, where α, p are in Assumption 5.1 in [20], i.e., test functions, by composing the inverse of a parameterization with Hermite bases, are H^1 on the physical domain. If we represent a parameterization $\mathcal{P}(s, t)$ with the combination of Bezier polynomials on each cells with one extraordinary vertex \mathbf{O} , the positions of control points referred to Assumption 5.1 in [20] are determined by $\frac{\partial^2 \mathcal{P}}{\partial s^2} |_{\mathbf{O}}, \frac{\partial^2 \mathcal{P}}{\partial t^2} |_{\mathbf{O}}, \frac{\partial^3 \mathcal{P}}{\partial s^2 \partial t} |_{\mathbf{O}}$ and $\frac{\partial^3 \mathcal{P}}{\partial s \partial t^2} |_{\mathbf{O}}$. Thus, during the subdivision, \mathcal{P} satisfies Assumption 5.1 in [20] over the finer parameter mesh if \mathcal{P} satisfies this integrability assumption over the initial parameter mesh.

In the following, we present two examples of parameterization with extraordinary points and show the results of numerical experimentation for the solution of Grad-Shafranov equations. During the subdivision of the parameter mesh, the parameterization does not change and the initial parameterizations satisfy Assumption 5.1 in [20]. All of the physical domains of these examples can be exactly described by Hermite bases. Thus, the errors come from approximation by Hermite bases. In Example 5.1, we take $g(r) \equiv 1$ and $f(u, r, z) = f(r, z)$ in the model PDE (24). In Example 5.2, $g(r) = 1/(r+2)^2$ and $f(u, r, z) = f(r, z) + u^2$, where $f(r, z)$ will be defined in Example 5.2. The exact solutions in Examples 5.1 and 5.2 are $C^4(\Omega)$.

Example 5.1.

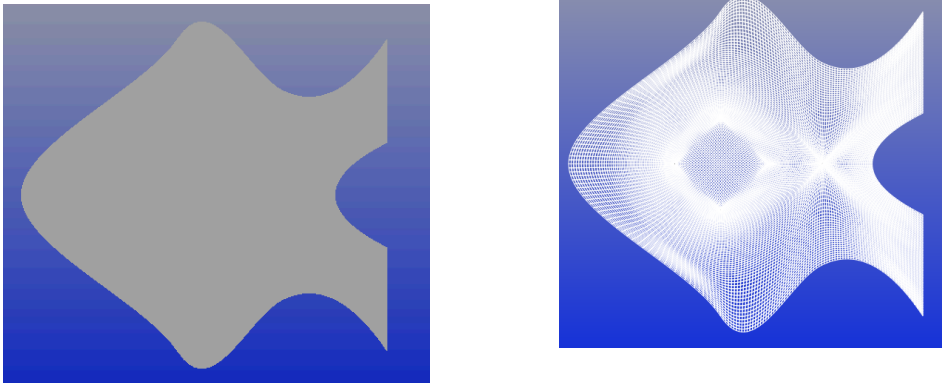


Figure 11: The physical domain and the parameterization of Example 5.1

1. The physical domain is shown on the left side of Figure 11, and its boundary is composed of the solutions of nine implicit bicubic polynomials, i. e., there are $F_1(r, z), F_2(r, z), \dots, F_9(r, z)$, which are bicubic polynomials, such that the boundary of this physical domain is a part of the solution of the following system:

$$\begin{cases} F_1(r, z) = 0 \\ F_2(r, z) = 0 \\ \dots\dots\dots \\ F_9(r, z) = 0 \end{cases}$$

2. The initial parametric mesh has the same topology as the “usual” mesh shown in Figure 12.

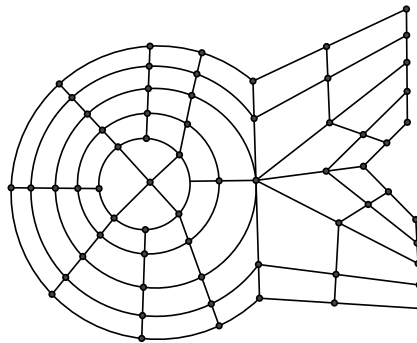


Figure 12: The “usual” mesh that has the same topology as the initial parametric mesh of Example 5.1

3. Take $g(r) \equiv 1$, and taking the exact solution of the model PDE (24) as $u = (r + 2)(r + 1)\prod_i^9 F_i(r, z)/10000$. Then, the right side term is $f(r, z) = -\Delta u$, i. e., the

PDE is

$$\begin{aligned} -\Delta u &= f \text{ in } \Omega; \\ u &= 0 \text{ on } \partial\Omega. \end{aligned}$$

Moreover, the initial parameterization of the physical domain is shown on the right side of Figure 11 with the exact boundary representation of the physical domain;

We globally refine the spline space by recursively splitting each of the original cells of the mesh into four subcells. In Figure 13, there are errors measured by L^2 -norm and H^1 -norm.

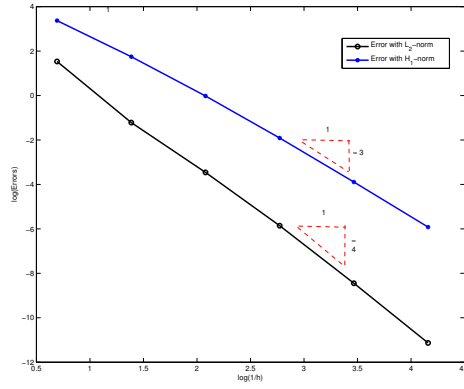


Figure 13: Errors with the L^2 -norm and H^1 -norm

Example 5.2.

1. The physical domain is the square $\Omega = [-1, 1] \times [-1, 1] \subset \mathbb{R}^2$;
2. We take $g(r) = 1/(r+2)^2$ $f(u, r, z) = G(r, z) + u^2$ so that the exact solution of the model PDE (24) is $u = (1 - r^2)(1 - z^2)$, where $G(r, z) = -(1 - r^2)^2(1 - z^2)^2 + 2(1 - z^2) - 8(1 - z^2)/(r + 2) - 2(1 - r^2)$. Under these conditions, the PDE is

$$\begin{aligned} -(r+2)^2 \nabla(R(r)\nabla u) &= -G(r, z) - u^2 \text{ in } \Omega, \\ u &= 0 \text{ on } \partial\Omega, \end{aligned}$$

where

$$R(r) = \begin{pmatrix} 1/(r+2)^2 & 0 \\ 0 & 1/(r+2)^2 \end{pmatrix}.$$

3. The initial parametric mesh has the same topology as the “usual” mesh shown in Figure 14;
4. The parameterization of Ω (with an exact boundary representation) is described in Figure 15.

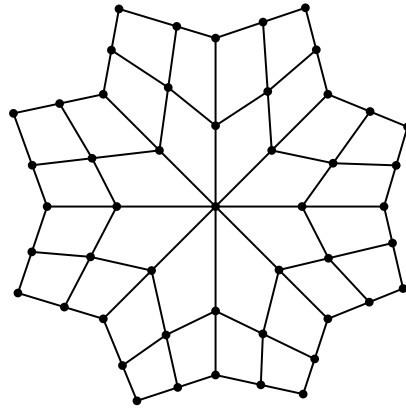


Figure 14: The “usual” mesh that has the same topology as the initial parametric mesh of Example 5.2

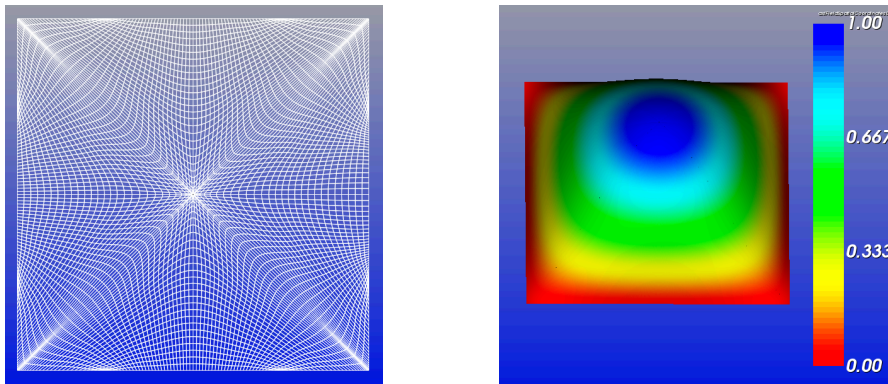


Figure 15: The parameterization of Ω and the isogeometric solution

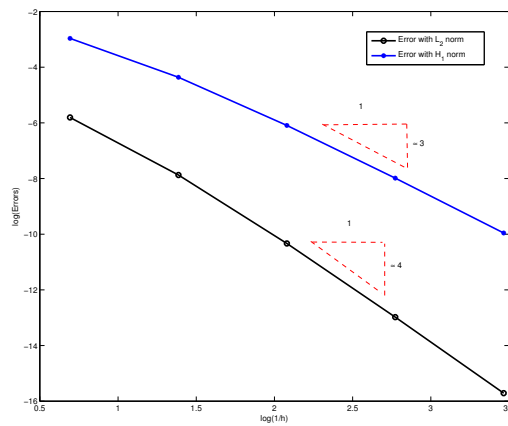


Figure 16: Errors with the L^2 -norm and H^1 -norm

We globally refine the spline space by recursively splitting each of the 8 cells of the mesh into four subcells. In Figure 16, there are errors measured by L^2 -norm and H^1 -norm.

For Examples 5.1 and 5.2, the error order with L^2 -norm is approximately 4 and that with H^1 -norm is approximately 3. That means, by these numerical examples, the optimal error orders are reached.

6. Conclusion and future work

This paper presents the definition of spline spaces over rectangular meshes with arbitrary topologies. A rule for local refinement of parametric meshes is presented, and the changes in spline space over these refined parametric meshes were studied by taking transition maps as rigid transformations. Especially, the property of bi-cubic spline spaces with C^1 parameter continuity is studied in detail for using it to solve PDE problems over a physical domain with a general topology. Concretely, the dimension formulae are given. Its basis functions called Hermite bases are also constructed. The results about properties for solving PDEs are in the following list.

1. C^1 continuity of test functions on a physical domain: the continuity of test functions is determined by the parameter continuity of splines and the property of parameterizations. We analyze the continuity of test functions obtained by composing the inverse of an H^1 -parameterization in [28] with Hermite bases. Although isolated singularities at extraordinary vertices of parameterizations, in Theorem 4.3, most of test functions are C^1 on the physical domain and the area of supports of essential H^1 -test functions has the same order as the interpolation approximation error order in Theorem 5.1. Moreover, a C^1 -constraint condition at extraordinary vertices is presented, i.e. by set the coefficients of these essential H^1 -test functions as zeros, such that all test functions are C^1 on a physical domain.
2. Theorem 5.1 presents the interpolation approximation L^2 error by Hermite bases. This error order is optimal. In the proof of this theorem, the coefficients of essential H^1 -test functions are zeros. Thus, the optimal interpolation approximation is still obtained C^1 -constraint condition at extraordinary vertices even if there is an additional C^1 -constraint condition at extraordinary vertices.
3. The numerical convergence rates for solving the Grad-Shafranov equation are analyzed. In the numerical experiments, optimal convergence rates with L^2 -norm and H^1 -norm are reached.

For a better solution of the MHD simulation over a general physical domain, further investigations are considered in the following directions:

- we need to generate a parameterization by Hermite bases that satisfies integrability assumptions, improving the quality of stiffness matrix. It has presented in our recent work [28];
- a parameterization algorithm should be developed for a better approximation of the boundaries of physical domains.

For other applications, splines with bi-degree (d, d) and C^r parameter continuity can be developed to solving PDEs over a complex physical domain.

Reference

- [1] O. Czarny and G. Huysmans. Bézier surfaces and finite elements for MHD simulations. *Journal of Computational Physics*, vol. 227, p. 7423–7445, 2008.
- [2] I. Ergatoudis, B. Irons, and O. Zienkiewicz. Curved isoparametric "quadrilateral" elements for finite element analysis. *Int. J. Solids Structures*, vol. 4, p. 31–42, 1968.
- [3] T. J. R. Hughes, J. A. Cottrell and Y. Bazilevs "Isogeometric analysis: CAD, finite elements, NURBS, exact geometry and mesh refinement". *Computer Methods in Applied Mechanics and Engineering*, vol. 194, Issues. 39-41, p. 4135–4195, 2005.
- [4] K. Höllig. *Finite Element Methods with B-Splines*. SIAM, 2003.
- [5] D. R. Forsey and R. H. Bartels. Hierarchical B-spline refinement. In *Proceedings of the 15th annual conference on Computer graphics and interactive techniques*, SIGGRAPH '88, pages 205–212, New York, NY, USA, 1988. ACM.
- [6] R. Kraft, Adaptive and linearly independent multilevel B-splines. In *Surface Fitting and Multiresolution Methods*, A. L. Méhauté, C. Rabut, and L. L. Schumaker, Eds., vol. 2. Vanderbilt University Press, p. 209 – 216.
- [7] C. Giannelli, B. Jüttler, and H. Speleers. THB-splines: The truncated basis for hierarchical splines. *Computer Aided Geometric Design*, 29(7):485 – 498, 2012.
- [8] T. Dokken, T. Lyche, and K. Pettersen. Polynomial splines over locally refined box-partitions. *Computer Aided Geometric Design*, 30(3), p. 331–356, 2013.
- [9] T. W. Sederberg, J. Zheng, A. Bakenov, A. Nasri. T-splines and T-NURCCs. *ACM Trans. Graph.*, vol. 22, p. 161–172, 2003.
- [10] X. Gu, Y. He, H. Qin, Manifold splines. *Graphical Models*, vol. 68, p. 237–254, 2006.
- [11] Y. He, K. Wang, H. Wang, X. Gu, H. Qin, Manifold T-spline. *Geometric Modeling and Processing-GMP 2006, Lecture Notes in Computer Science*, vol. 4077, p. 409–422, 2006.
- [12] H. Wang, Y. He, X. Li, X. Gu, H. Qin, Polycube Splines. *Computer-Aided Design*, vol. 40, p. 721–733, 2008.
- [13] L. Ying, D. Zorin, A simple manifold-based construction of surfaces of arbitrary smoothness. *ACM Trans. Graph.*, vol. 23, p. 271–275, 2004.

- [14] J. Peter, U. Reif, Subdivision Surfaces. *Geometry and Computing, Springer-Verlag*, ISBN 878-3-540-76406-9, 2008.
- [15] G. T. A. Huysmans, J. P. Goedbloed. “Isoparametric Bicubic Hermite Elements for Solution of the Grad-Shafranov Equation”. *International Journal of Modern Physics C*, p. 371-376, 1991.
- [16] K. H. Huebner, E. A. Thornton. The Finite Element Method for Engineers. *John Wiley & Sons*, ISBN 0-471-09159-6, 1982.
- [17] J. Deng, F. Chen, and Y. Feng. Dimensions of spline spaces over T-meshes. *Journal of Computational and Applied Mathematics*, vol. 194, p. 267–283, 2006.
- [18] L. L. Schumaker and L. Wang. Approximation power of polynomial splines on T-meshes *Computer Aided Geometric Design* 29, p. 599 – 612, 2012
- [19] Xin Li, Jiansong Deng, Falai Chen “Polynomial splines over general T-meshes”. *The Visual Computer*, vol. 26, p. 277-286, 2009.
- [20] T. Takacs, B. Jüttler. “Existence of Stiffness Matrix Integrals for Singularly Parameterized Domains in Isogeometric Analysis”. *Computer Methods in Applied Mechanics and Engineering*, vol. 200, p. 3568–3582, 2011.
- [21] T. Takacs, B. Jüttler. “ H^2 regularity properties of singular parameterizations in isogeometric analysis”. *Graphical Models*, vol. 74, p. 361–372, 2012.
- [22] A. Quarteroni, A. Valli. Numerical Approximation of Partial Differential Equations. *Springer-Verlag*, ISBN 3-540-57111-6, 1997.
- [23] L. L. Schumaker, L. Wang. On Hermite interpolation with polynomial splines on T-meshes. *Journal of Computational and Applied Mathematics*, vol. 240, p. 42–50, 2013.
- [24] A. Pataki, A. J. Cerfon, J. P. Freidberg, L. Greengard and M. O. Neil. A fast, high-order solver for the Grad-Shafranov equation. *J. Comput. Phys.*, vol. 243, p. 28–45, 2013.
- [25] B. Mourrain. On the dimension of spline spaces on planar T-meshes. *Mathematics of Computation*, 83, p. 847–871, 2014.
- [26] R. L. Burden, J. D. Faires. Numerical Analysis. *Prindle, Weber and Schmidt*, Boston, MA 1985.
- [27] J. Lu “Circular element: Isogeometric elements of smooth boundary’. *Computer Methods in Applied Mechanics and Engineering*, vol. 198, p. 2391–2402, 2009.
- [28] M. Wu, B. Mourrain, A. Galligo and B. Nkonga. “ H^1 -parameterizations of plane physical domains with complex topology in Isogeometric analysis”. *submitted to Computational Mechanics*, <https://hal.archives-ouvertes.fr/hal-01196435/>.